

## **Supporting Information**

### **Photoinduced Electron Transfer and Changes in Surface Free Energy in Polythiophene-Polyviologen Bilayered Thin Films**

Mary K. Danielson, Jie Chen, Anna K. Vaclavek, Nathan D. Colley, Abdul-Haq Alli,  
Richard A. Loomis, Jonathan C. Barnes\*

*Department of Chemistry, Washington University, St. Louis, MO 63130, USA*

\*E-mail: jcbarnes@wustl.edu



## Table of Contents

<b>Section A. Materials / General Methods / Instrumentation.....</b>	<b>S3</b>
<b>Section B. Synthesis of Polythiophene and Viologen-based Crosslinker.....</b>	<b>S6</b>
1) Synthesis of 3-thienylethanamine.....	S6
2) Synthesis of dimethyl 3,3'-((2-(thiophen-3-yl)ethyl)azanediyl)dipropionate.....	S7
3) Synthesis of poly(3,3'-((2-(thiophen-3-yl)ethyl)azanediyl)dipropionic acid).....	S8
4) Synthesis of HEG-BIPY <sup>2+</sup> (2V·2OTs).....	S9
5) Synthesis of 2V-St·2OTs·2Cl: Styrene-Capped Dimer Crosslinker.....	S10
<b>Section C. Methods for Bilayered Thin-Film Fabrication.....</b>	<b>S11</b>
1) Polythiophene (PTh) Bottom-Layer Film Fabrication.....	S11
2) Polyviologen (PV) Crosslinked Top-Layer Film Fabrication.....	S11
<b>Section D. Electrochemical Characterization of Bilayered Thin-Films.....</b>	<b>S15</b>
<b>Section E. Physical and Morphological Characterization of Bilayered Thin-Films.....</b>	<b>S17</b>
1) Contact Angle Measurements.....	S17
2) Profilometry .....	S19
3) Atomic Force Microscopy.....	S22
4) Scanning Electron Microscopy.....	S24
5) Gel Permeation Chromatography.....	S25
6) <sup>1</sup> H NMR Spectroscopy.....	S26
<b>Section F. UV-Vis-NIR Absorption / Photoluminescence Spectroscopy.....</b>	<b>S27</b>
1) UV-Vis-NIR Absorption Spectra.....	S27
2) Photoluminescence Spectra.....	S28
<b>Section G. Femtosecond Transient Absorption Spectroscopy.....</b>	<b>S29</b>
1) Fitting of Temporal Profiles .....	S30
2) Dependence of fTA data on Excitation Fluence .....	S34
3) Dependence of fTA Data on Excitation Time .....	S35
<b>Section H. References.....</b>	<b>S36</b>



## Section A. Materials / General Methods / Instrumentation

All reagents were purchased from commercial suppliers and used without further purification. Literature procedures were utilized in the syntheses of hexaethylene glycol di-*p*-toluenesulfonate (**HEG-Tos**),<sup>S1</sup> HEG-BIPY<sup>2+</sup> (**2V**·2OTs),<sup>S2</sup> styrenated HEG-BIPY<sup>4+</sup> (**2V-St**·2OTs·2Cl),<sup>S2</sup> 3-thienylethanamine,<sup>S3</sup> dimethyl 3,3'-((2-(thiophen-3-yl)ethyl)azanediyl)dipropionate,<sup>S4</sup> and poly(3,3'-((2-(thiophen-3-yl)ethyl)azanediyl)dipropionic acid) (**PTh**).<sup>S4</sup> Column chromatography was carried out on any synthesized compounds using silica gel for chromatography from Sorbtech. Spectra/Por dialysis membrane, pre-treated RC tubing dialysis bags were acquired from Spectrum. A Thermo Scientific Sorvall ST 8 small benchtop centrifuge was used during synthesis of the **2V-St**·2OTs·2Cl crosslinker. All nuclear magnetic resonance (NMR) spectra were recorded on Varian Inova-500 and Varian Mercury 300 spectrometers at 25 °C, with working frequencies of 500 (<sup>1</sup>H) and 125 (<sup>13</sup>C) MHz and 300 (<sup>1</sup>H) and 75 (<sup>13</sup>C) MHz, respectively. Low resolution mass spectrometry (LRMS) was performed using an Advion Expression mass spectrometer. The reported chemical shifts are given in ppm relative to residual non-deuterated solvents: (CH<sub>3</sub>)<sub>2</sub>SO, and CH<sub>2</sub>Cl<sub>2</sub>. The thin films were all prepared utilizing a Brewer Science CEE 200X spin-coater inside a 10,000-class clean room. The substrates for all films were 1 in x 1 in cut sodium silicate microscope slides. The slides were cleaned in a MeOH bath and dried with a lint-free cloth before coating. All films were purged of O<sub>2</sub> after fabrication by placing inside a plastic container and applying a strong stream of N<sub>2</sub> for 1 d. A petri dish of H<sub>2</sub>O was also placed inside the box to prevent the films from drying out during these purging sessions. The thickness of the films was determined by making a thick scratch in the films with the back of a razor blade followed by obtaining topographical data from a KLA-Tencor Alpha-Step D-100 Profilometer. Thickness of the two individual layers was determined first by measuring the thickness of the **PTh** layer, then the thickness of the bilayers. The thickness of the top layer could then be determined through subtraction. Any reduction and excitation of the films prior to contact angle measurements was



induced through exposure to 450 nm (blue), 36W light with a fluence of 0.32 J/cm<sup>2</sup>. The light source was placed 3 in from the top of the film. Ultraviolet-Visible-Near Infrared (UV-Vis-NIR) absorbance spectra were acquired using an Agilent Cary 5000 spectrophotometer with a PbSmart NIR detector. Electrochemistry experiments were conducted on a Gamry multipurpose potentiostat. Linear sweep voltammetry experiments were conducted on three films (PTh, PV, and bilayered) following the fabrication procedure for the PTh film, the 1.5 μm PV layer, and the 1.5 μm bilayered film using an indium tin oxide (ITO) slide as substrate as the working electrode. This is in place of the sodium silicate microscope slide used for imaging and contact angle measurements. Imaging of the films was completed on a Thermo Quattro S environmental scanning electron microscope (ESEM) in low vacuum mode. Topographical data was collected from a Bruker Dimensions ICO Atomic Force Microscope (AFM) using a ScanAsyst-Air AFM tip with a scanning rate of 1.0 Hz. Optical microscopy was obtained using an Evos XL Core microscope. Contact angle images were acquired through use of a Samsung Note 10+ as camera with a Clarus 15x macro lens attachment. Images were captured at 1 s after dropping 1.5 μL of solvent onto the film. All images were analyzed in ImageJ and all contact angles ( $\Theta_E$ ) are reported. The femtosecond TA (fTA) experiments were performed using the output of a commercial Ti: sapphire amplifier laser system (800 nm, ~2.3 Watts at 1 kHz, and ~120 fs pulse width) and a commercial fTA spectrometer. A fraction of the laser output was focused into a sapphire crystal to generate a white light continuum (450-760 nm) for use as the probe beam. The remainder of the laser output pumped a commercial optical parameter amplifier to provide excitation pulses at either 500 nm (2.48 eV) or 450 nm (2.76 eV) with a bandwidth of ~12 nm. A motorized delay stage was used to control the delay time between the pump and probe pulses,  $t$ , with  $t < 1.5$  ns. The data were collected for 2 s at each  $t$ . The unpolarized excitation and probe beams were gently focused on the sample, which was positioned orthogonally to the probe beam path. The excitation fluence was kept to ~50 μJ cm<sup>-2</sup> pulse<sup>-1</sup> to minimize multi-carrier interactions and heating effects. Some fTA data were collected at higher excitation fluences to identify possible differences, no



changes were observed. TA data were typically collected with nitrogen purge to minimize contributions from oxygen, but also under ambient air conditions.

fTA spectroscopy is a differential absorption ( $\Delta Abs$ ) measurement, where the broad, probe continuum is used to monitor changes in the absorption spectra of the sample with and without excitation as a function of  $t$  after photoexcitation. For a single measurement at a given  $t$ , two transmission spectra of the probe laser are collected. One spectrum is recorded by acquiring the spectral profile of the probe laser pulse with the excitation beam blocked,  $T_{pr}(E)$ . A second transmission spectrum is acquired with the excitation laser pulse traversing the sample at  $t$  before the probe pulse,  $T_{Exc+pr}(E, t)$ . The differential absorption is then given by:

$$\Delta Abs(E, t) = \log_{10} \left( \frac{T_{pr}(E)}{T_{Exc+pr}(E, t)} \right).$$

In terms of the absorption spectra of the excited and unexcited sample, this equation is rearranged to yield:

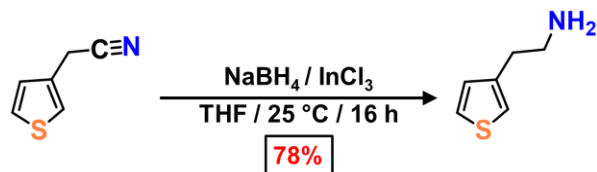
$$\Delta Abs(E, t) = Abs_{Exc+pr}(E, t) - Abs_{pr}(E).$$

Thus,  $\Delta Abs(E, t)$  spectra are collected at half of the repetition rate of the laser, at 500 Hz. Due to the broad spectral profile of the probe pulses and the wavelength dependence of the index of refraction of the sample, the data were corrected for the spectral chirp using the data collection software. Ultimately, the temporal width of the instrument response function was ~200 fs for these fTA measurements.



## Section B. Synthesis of Polythiophene and Viologen-based Crosslinker

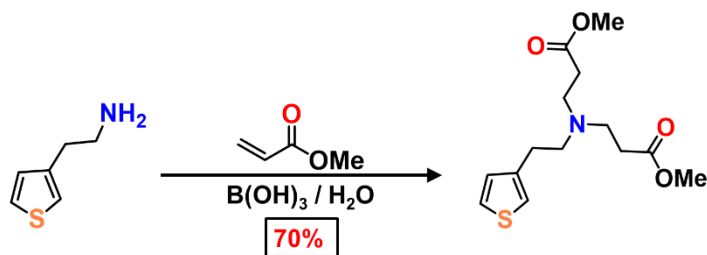
### 1) Synthesis of 3-thienylethanamine



The 3-thienylethanamine<sup>S3</sup> was synthesized following a reported literature procedure.  $\text{NaBH}_4$  (1.00 g, 27.12 mmol, 3 equiv) and  $\text{InCl}_3$  (1.97 g, 8.94 mmol, 1 equiv) were added to an oven dried 100 mL round-bottom flask. Anhydrous THF (30 mL) was added to the flask. The mixture was allowed to stir under  $\text{N}_2$  for 30 min. Then, 3-thiophene acetonitrile (1.02 mL, 8.94 mmol, 1 equiv) was added to the flask dropwise. The mixture was allowed to stir at  $25^\circ\text{C}$  for 16 h. After this time, the  $\text{NaBH}_4$  was neutralized with 20 mL of 2.8 M HCl. This mixture was refluxed for 2 h, or until gray precipitate was dissolved. Next, 10 mL of MeOH were added to the flask and the mixture was allowed to reflux for another 2 h. After this, the approximately 10 mL of methyl-borate MeOH were removed through evaporation. The mixture was washed three times with 10 mL of  $\text{CH}_2\text{Cl}_2$ . The aqueous layer was then basified through addition of concentrated NaOH in  $\text{H}_2\text{O}$  to a pH of 12. The white precipitate was filtered away and the mixture was extracted three times with 10 mL of  $\text{CH}_2\text{Cl}_2$ . The  $\text{CH}_2\text{Cl}_2$  was evaporated to yield 0.89 g (78%) of 3-thienylethanamine.  $^1\text{H}$  NMR (500 MHz,  $\text{CD}_2\text{Cl}_2$ )  $\delta$  7.30 (dd,  $J = 4.9, 3.0$  Hz, 1H), 7.03 (d,  $J = 2.0$  Hz, 1H), 7.00 (d,  $J = 4.9$  Hz, 1H), 2.93 (t,  $J = 6.8$  Hz, 2H), 2.77 (t,  $J = 6.8$  Hz, 2H), 1.23 (s, 2H).  $^{13}\text{C}$  NMR (500 MHz,  $\text{CD}_2\text{Cl}_2$ )  $\delta$  140.7, 128.3, 125.3, 120.8, 42.9, 34.6. LRMS (ESI):  $m/z$  calculated for  $\text{C}_6\text{H}_{11}\text{NS}$  [ $M + \text{H}$ ] $^+$  127.1 amu, found [ $M + \text{H}$ ] $^+$  127.1 amu.



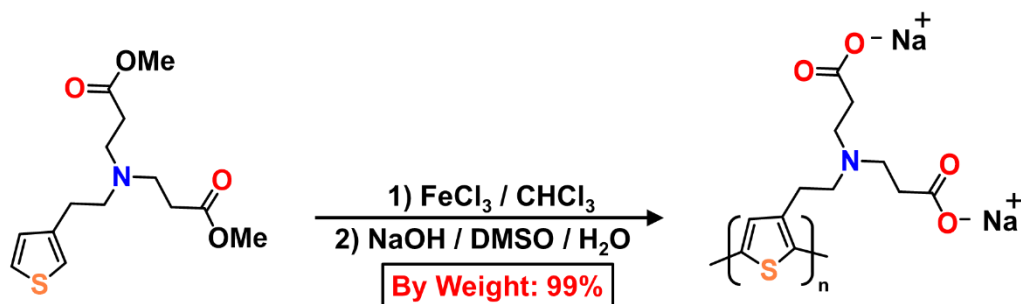
## 2) Synthesis of dimethyl 3,3'-((2-(thiophen-3-yl)ethyl)azanediyl)dipropionate



The dimethyl 3,3'-((2-(thiophen-3-yl)ethyl)azanediyl)dipropionate<sup>S4</sup> was synthesized according to a literature procedure. The 3-thienylethanamine (1.14 g, 6.96 mmol, 1 equiv) was dissolved in 10 mL of MeOH and added to a 100 mL round-bottom flask. Then, methyl acrylate (3.15 mL, 34.8 mmol, 5 equiv) was dissolved in 5 mL of MeOH and added to the reaction flask. Boric acid (0.04 g, 0.70 mmol, 0.1 equiv) was dissolved in 3 mL of H<sub>2</sub>O and added to the reaction flask. The mixture was capped and heated to 37 °C for 12 h. The MeOH was then evaporated, and the product was run through a silica gel column packed in 4:1 hexanes: EtOAc eluent and flushed with the same. This yielded 1.45 g (70%) of the product as a light-yellow oil. <sup>1</sup>H NMR (500 MHz, CD<sub>2</sub>Cl<sub>2</sub>) δH 7.27 (dd, *J* = 4.9, 3.0 Hz, 1H), 7.02 (d, *J* = 1.9 Hz, 1H), 6.98 (dd, *J* = 4.9, 1.2 Hz, 1H), 3.66 (s, 6H), 2.84 (t, *J* = 7.0 Hz, 4H), 2.75 (dt, *J* = 14.0, 6.6 Hz, 4H), 2.46 (t, *J* = 7.0 Hz, 4H). <sup>13</sup>C NMR (125 MHz, CD<sub>2</sub>Cl<sub>2</sub>): δC 172.7, 128.4, 125.0, 120.6, 54.6, 51.3, 49.2, 32.5, 28.1. LRMS (ESI): *m/z* calculated for C<sub>14</sub>H<sub>22</sub>NO<sub>4</sub>S [*M* + H]<sup>+</sup> 300.1 amu, found 299.9 [*M* + H]<sup>+</sup> amu.



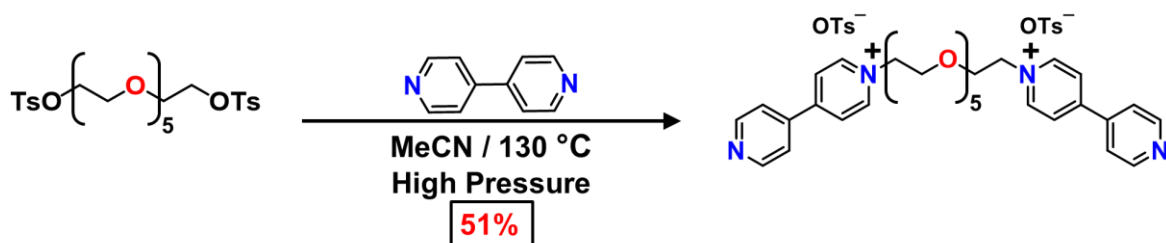
### 3) Synthesis of poly(3,3'-((2-(thiophen-3-yl)ethyl)azanediyl)dipropionic acid)



Poly(3,3'-((2-(thiophen-3-yl)ethyl)azanediyl)dipropionic acid) (**PTh**) was prepared following a reported literature procedure.<sup>S4</sup> FeCl<sub>3</sub> (3.15 g, 19.47 mmol, equiv) was added to a 200 mL round-bottom flask and suspended in 50 mL of CHCl<sub>3</sub>. Then, the mixture was allowed to stir at room temperature for 30 min. After 30 min, the monomer (1.46 g, 4.87 mmol, 1 equiv) was dissolved in 5 mL of CHCl<sub>3</sub> and added dropwise to the reaction flask. The reaction was allowed to stir at room temperature for 2 d. After this time, 10 mL of MeOH were added to the flask. A thick black oil precipitated out of solution. The precipitate was collected and washed with 200 mL of a 1:1 mixture of CHCl<sub>3</sub>: MeOH. The precipitate was then dissolved in 10 mL of DMSO and added to a small 50 mL round-bottom flask. Then 30 mL of 3M aqueous NaOH solution were added to the flask. The reaction was heated to 50 °C and allowed to stir for 12 h. After 12 h, the reaction mixture was transferred to a dialysis bag (MW cutoff 1 kD) and dialyzed for 2 d in de-ionized H<sub>2</sub>O. The resulting product from the dialysis bag was filtered. The H<sub>2</sub>O was evaporated to yield 3.12 g (99% by weight) of the water-soluble **PTh**. <sup>1</sup>H NMR (300 MHz, D<sub>2</sub>O) δH 7.27 (bs), 4.66 (bs), 3.28 (bs), 2.46 (bs).



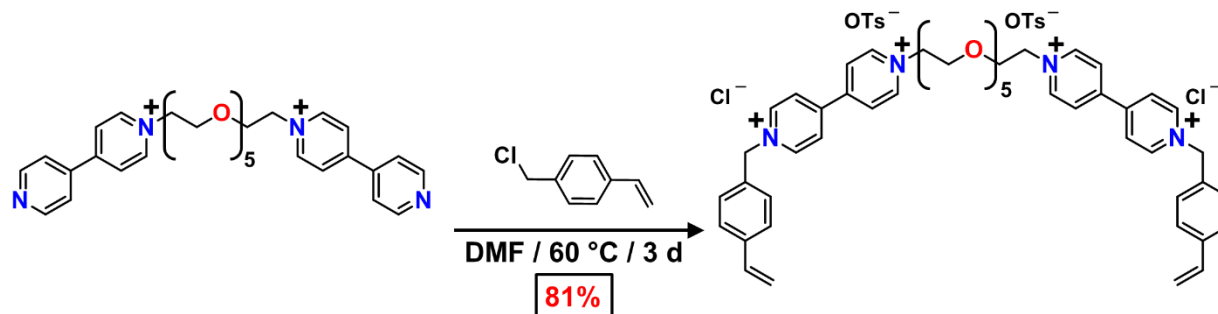
#### 4) Synthesis of HEG-BIPY<sup>2+</sup> (**2V**·2OTs)



HEG-BIPY<sup>2+</sup> (**2V**·2OTs)<sup>S2</sup> was synthesized according to the literature procedure reported by our group. **HEG-Tos** (1.5 g, 2.5 mmol, 1 equiv) and 4,4'-bipyridine (7.93 g, 50 mmol, 20 equiv) were dissolved in MeCN (dry, 15 mL) and the solution was added to a 100 mL thick-walled high-pressure flask with a Teflon screw cap and stir bar. The flask was capped tightly, and the mixture was heated to 130 °C for 16 h (high pressure). After 16 h, the solution was transferred to four 50 mL centrifuge tubes and diluted to 50 mL with PhMe to precipitate the product. The tubes were centrifuged at 4500 RPM at −10 °C for 30 min. The resulting supernatant was decanted, the dark brown oil was re-dissolved in 5 mL MeCN and 45 mL PhMe was added, followed by centrifugation. This process was repeated three times to yield 1.8 g (51%) of the desired product, **2V**·2OTs, as a viscous, brown solid. <sup>1</sup>H NMR (500 MHz, (CD<sub>3</sub>)<sub>2</sub>SO): δH 9.15 (d, *J* = 7.0 Hz, 4H); 8.86 (dd, *J* = 4.5, 1.7 Hz, 4H); 8.62 (d, *J* = 7.0 Hz, 4H); 8.03 (dd, *J* = 4.5, 1.7 Hz, 4H); 7.50 – 7.46 (m, 4H); 7.09 (d, *J* = 7.8 Hz, 4H); 4.82 (t, *J* = 4.9 Hz, 4H); 3.93 (t, *J* = 4.9 Hz, 4H); 3.56 – 3.50 (m, 4H); 3.45 – 3.35 (m, 12H); 2.27 (s, 6H). <sup>13</sup>C NMR (125 MHz, (CD<sub>3</sub>)<sub>2</sub>SO): δC 152.4, 150.8, 145.8, 145.8, 140.9, 137.5, 128.0, 125.5, 125.0, 121.9, 69.6, 69.59, 69.58, 69.4, 68.6, 59.9, 20.7. LRMS (ESI): *m/z* calculated for C<sub>46</sub>H<sub>54</sub>N<sub>5</sub>S<sub>2</sub>O<sub>11</sub> [*M* – 2OTs]<sup>2+</sup> 280.2 amu, found 280.1 [*M* – 2OTs]<sup>2+</sup> amu.



### 5) Synthesis of 2V-St-2OTs-2Cl: Styrene-Capped Dimer Crosslinker

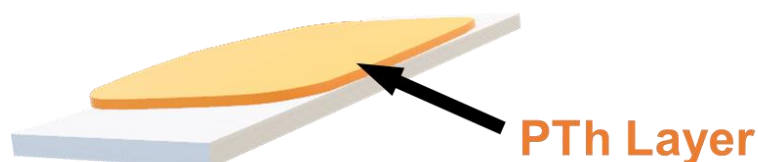


Styrenated HEG-BIPY<sup>4+</sup> (**2V-St-2OTs-2Cl**)<sup>S2</sup> was synthesized according to a previously reported literature procedure. **2V-2OTs** (1.6 g, 1.8 mmol, 1 equiv)<sup>S2</sup> and 4-vinylbenzyl chloride (11.0 g, 72 mmol, 40 equiv) were dissolved in MeCN (dry, 40 mL, 40 mg·mL<sup>-1</sup> **2V-2OTs**) and heated to 55 °C for 72 h. After 72 h, MeOH (10 mL) was added to the solution to dissolve the precipitate and the solution was transferred to four 50 mL centrifuge tubes and diluted with 40 mL PhMe to precipitate the product. The tubes were centrifuged at 4500 RPM at -10 °C for 30 min. The resulting supernatant was decanted, and the viscous, brown oil was washed by adding 50 mL MeCN to each tube, followed by sonication and centrifugation. The supernatant was decanted, and this process was repeated three times. The oil was then dissolved in 5 mL MeOH and precipitated a final time by adding 50 mL 1:1 PhMe: Et<sub>2</sub>O to yield 0.8g (81%) of the desired product, **2V-St-2OTs-2Cl**, as a dark brown, viscous solid. <sup>1</sup>H NMR (500 MHz, (CD<sub>3</sub>)<sub>2</sub>SO): δH 9.65 (d, *J* = 6.4 Hz, 4H); 9.40 (t, *J* = 8.5 Hz, 4H); 8.93 – 8.76 (m, 8H); 7.66 (d, *J* = 8.1 Hz, 4H); 7.55 (d, *J* = 8.1 Hz, 4H); 7.47 (d, *J* = 7.9 Hz, 4H); 7.08 (d, *J* = 7.8 Hz, 4H); 6.74 (dd, *J* = 17.6, 11.0 Hz, 2H); 6.02 (s, 4H); 5.91 (t, *J* = 16.4 Hz, 2H); 5.32 (d, *J* = 11.0 Hz, 2H); 4.97 – 4.88 (m, 4H); 4.02 – 3.90 (m, 4H); 3.61 – 3.52 (m, 4H); 3.49 – 3.31 (m, 5H); 2.26 (s, 1H). <sup>13</sup>C NMR (125 MHz, (CD<sub>3</sub>)<sub>2</sub>SO): δC 149.0, 148.8, 146.2, 145.7, 145.6, 138.2, 137.6, 135.8, 133.6, 129.4, 128.0, 127.1, 126.8, 126.3, 125.4, 115.8, 69.6, 69.6, 69.5, 68.6, 62.9, 60.3, 20.7. LRMS (ESI): *m/z* calculated for C<sub>64</sub>H<sub>72</sub>Cl<sub>2</sub>N<sub>4</sub>O<sub>11</sub>S<sub>2</sub> [*M* – Cl – OTs]<sup>2+</sup> 500.2 amu, found [*M* – Cl – OTs]<sup>2+</sup> 500.2 amu.



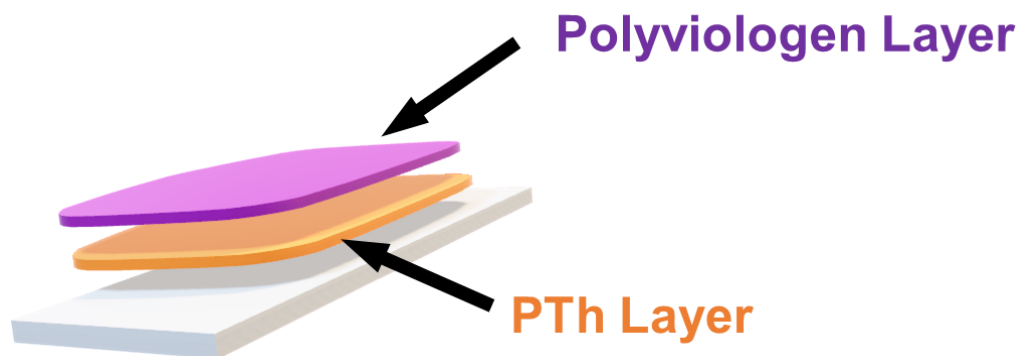
## Section C. Methods for Bilayered Thin-Film Fabrication

### 1) Polythiophene (PTh) Bottom-Layer Film Fabrication



A  $60 \text{ mg} \cdot \text{mL}^{-1}$  solution of **PTh** was made using a 1:1 mixture of MeOH and  $\text{H}_2\text{O}$ . To generate the bottom layer, the 1 in x 1 in glass slide was heated to  $125^\circ\text{C}$  using a hot-plate. The hot slide was then quickly transferred to the spin-coater and  $250 \mu\text{L}$  of the **PTh** mixture was deposited onto the slide. The slide was then spun for 2 s at 4500 RPM with a ramp speed of  $4500 \text{ RPM} \cdot \text{s}^{-1}$ . After spinning, the slide was placed back on the hot plate for 30 s to ensure even drying. This procedure resulted in films with an average thickness of  $0.23 \pm 0.03 \mu\text{m}$ .

### 2) Polyviologen (PV) Crosslinked Top-Layer Film Fabrication



#### Films of Average Thickness 0.5 and $1.5 \mu\text{m}$

75 mg of **2V-St**·2OTs·2Cl crosslinker was weighed and added into a 10 mL round-bottom flask. Then 1.25 mg of lithium phenyl-2,4,6-trimethylbenzoylphosphinate (LAP) was added to the



reaction flask. Then, 225  $\mu\text{L}$  of methacrylic acid and 75  $\mu\text{L}$  of deionized  $\text{H}_2\text{O}$  was added to the reaction flask. The mixture was sonicated to ensure that all crosslinker and initiator were dissolved. Then, the mixture was degassed through freeze-pump-thawing three times. Briefly, the reaction mixture was frozen in a small dewar filled with liquid  $\text{N}_2$ . After freezing, and while still submerged, a vacuum was applied to the reaction flask for 3 min. Then, the vacuum was removed, and the flask was extracted from the liquid  $\text{N}_2$  bath and allowed to thaw at room temperature. Small bubbles should appear as the solvent is degassed. This process is repeated twice more to ensure that all gas is eliminated from the reaction mixture. The mixture was then transferred into a clean room and plated on top of the **PTh**-coated substrate. 300  $\mu\text{L}$  of the **2V-St**-2OTs-2Cl mixture was plated onto the **PTh**-coated substrate on a spin-coater.

#### *0.5 $\mu\text{m}$ Conditions*

The substrate and monomer mixture were spun for 10 s at a velocity of 5000 RPM and ramp of 1000  $\text{RPM}\cdot\text{s}^{-1}$ , followed by a second step, spinning at 500 RPM with a ramp of 500  $\text{RPM}\cdot\text{s}^{-1}$  for 10 min. During spinning, the substrate was irradiated with a UV (365 nm) 75 W light source, placed 3 in from the top of the film. The average thickness of the top layer synthesized films is  $0.5 \pm 0.08 \mu\text{m}$ .

#### *1.5 $\mu\text{m}$ Conditions*

The substrate and monomer mixture were spun for 10 s at a velocity of 1000 RPM and ramp of 100  $\text{RPM}\cdot\text{s}^{-1}$ , followed by a second step, spinning at 500 RPM with a ramp of 500  $\text{RPM}\cdot\text{s}^{-1}$  for 10 min. During spinning, the substrate was irradiated with a UV (365 nm) 75 W light source, placed 3 in from the top of the film. The average thickness of the top layer synthesized films is  $1.5 \pm 0.6 \mu\text{m}$ .



#### Films of 4.0 $\mu\text{m}$ Average Thickness

75 mg of **2V-St**-2OTs-2Cl crosslinker was weighed and added into a 10 mL round-bottom flask. Then 1.25 mg of LAP were added, 257  $\mu\text{L}$  of methacrylic acid, and 43  $\mu\text{L}$  of deionized  $\text{H}_2\text{O}$  were added to the reaction flask. The mixture was sonicated to ensure that all crosslinker and initiator were dissolved. Then, the mixture was degassed through freeze-pump-thawing three times. Briefly, the reaction mixture was frozen in a small dewar filled with liquid  $\text{N}_2$ . After freezing, and while still submerged, vacuum was applied to the reaction flask for 3 min. Then, the vacuum was removed, and the flask was extracted from the liquid  $\text{N}_2$  bath and allowed to thaw at room temperature. Small bubbles should appear as the solvent is degassed. This process is repeated twice more to ensure that all gas is eliminated from the reaction mixture. The mixture was then transferred into a clean room and plated on top of the **PTh**-coated substrate. 300  $\mu\text{L}$  of the **2V-St**-2OTs-2Cl mixture was plated onto the **PTh**-coated substrate on a spin-coater. The substrate and monomer mixture were spun for at a velocity of 450 RPM and ramp of  $100 \text{ RPM}\cdot\text{s}^{-1}$  for 10 s, followed by a second step, spinning at 450 RPM with a ramp of  $500 \text{ RPM}\cdot\text{s}^{-1}$  for 10 min. During spinning, the substrate was irradiated with a UV (365 nm) 75 W light source, placed 3 in from the top of the film. The average thickness of the top layer synthesized films is  $4.0 \pm 0.8 \mu\text{m}$ .

#### Films of 6.0 $\mu\text{m}$ Average Thickness

75 mg of **2V-St**-2OTs-2Cl crosslinker was weighed and added into a 10 mL round-bottom flask. Then 1.25 mg of LAP were added, 225  $\mu\text{L}$  of methacrylic acid, and 75  $\mu\text{L}$  of deionized  $\text{H}_2\text{O}$  were added to the reaction flask. Then an additional 75  $\mu\text{L}$  of MeOH was added to the reaction flask. The mixture was sonicated to ensure that all crosslinker and initiator was dissolved. Then, the mixture was degassed through freeze-pump-thawing three times. Briefly, the reaction mixture was frozen in a small dewar filled with liquid  $\text{N}_2$ . After freezing, and while still submerged, vacuum was applied to the reaction flask for 3 min. Then, the vacuum was removed, and the flask was extracted from the liquid  $\text{N}_2$  bath and allowed to thaw at room temperature. Small bubbles should



appear as the solvent is degassed. This process is repeated twice more to ensure that all gas is eliminated from the reaction mixture. The mixture was then transferred into a clean room and plated on top of the **PTh**-coated substrate. 300  $\mu\text{L}$  of the **2V-St**-2OTs-2Cl mixture was drop-cast onto the **PTh**-coated substrate. The substrate was irradiated with a UV (365 nm) 75 W light source, placed 3 in from the top of the film, for 6 h to ensure complete polymerization. The average thickness of the top layer synthesized films is  $6.0 \pm 1.1 \mu\text{m}$ .

#### Films of 11.3 $\mu\text{m}$ Average Thickness

75 mg of **2V-St**-2OTs-2Cl crosslinker was weighed and added into a 10 mL round-bottom flask. Then 1.25 mg of LAP were added, 225  $\mu\text{L}$  of methacrylic acid, and 75  $\mu\text{L}$  of deionized  $\text{H}_2\text{O}$  were added to the reaction flask. The mixture was sonicated to ensure that all crosslinker and initiator was dissolved. Then, the mixture was degassed through freeze-pump-thaw methodology. Briefly, the reaction mixture was frozen in a small dewar filled with liquid  $\text{N}_2$ . After freezing, and while still submerged, vacuum was applied to the reaction flask for 3 min. The vacuum was removed, and the flask was then extracted from the liquid  $\text{N}_2$  bath and allowed to thaw at room temperature. Small bubbles should appear as the solvent is degassed. This process is repeated twice more to ensure that all gas is eliminated from the reaction mixture. The mixture was then transferred into a clean room and plated on top of the **PTh**-coated substrate. 300  $\mu\text{L}$  of the **2V-St**-2OTs-2Cl mixture was drop-cast onto the **PTh**-coated substrate. The substrate was irradiated with a UV (365 nm) 75 W light source, placed 3 in from the top of the film, for 6 h to ensure complete polymerization. The average thickness of the top layer synthesized films is  $11.3 \pm 1.1 \mu\text{m}$ .



## Section D. Electrochemical Characterization of Bilayered Thin-Films

All electrochemistry was conducted using a Ag/AgCl reference electrode in 1.0 M KCl in H<sub>2</sub>O and a Pt wire counter electrode. Arrows indicate points used to determine onset potential.

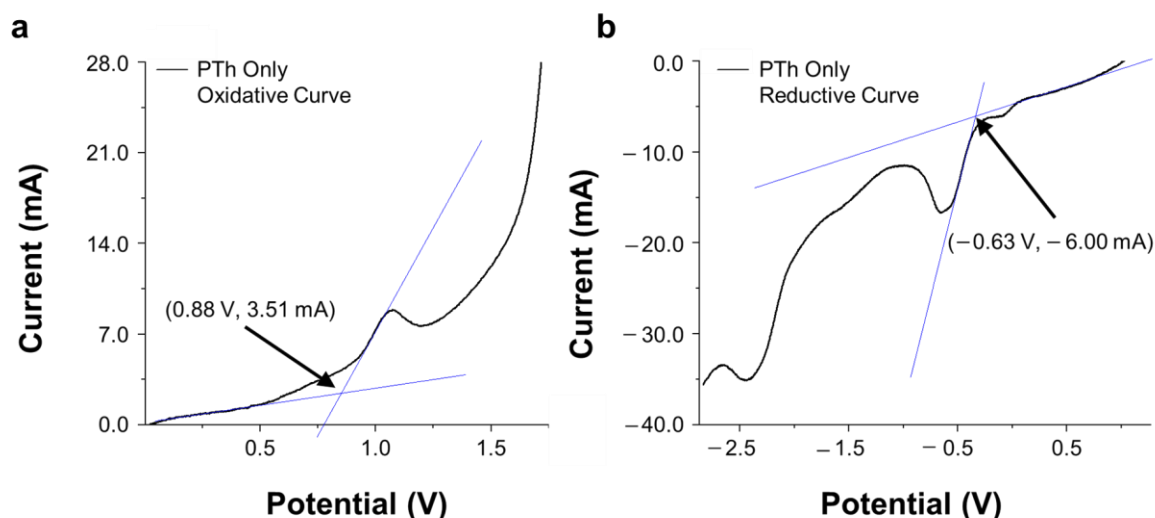


**Figure S1:** (a) Linear sweep voltammetry of 5  $\mu\text{L}$  of 60  $\text{mg}\cdot\text{mL}^{-1}$  solution of PTh in 1:1 H<sub>2</sub>O: MeOH mixture dropped onto glassy carbon electrode surface, starting voltage of 0.0 V, ending voltage of 1.75 V, 500  $\text{mV}\cdot\text{s}^{-1}$  scan rate in 0.1 M TBAPF<sub>6</sub> in DMF. (b) Linear sweep voltammetry of 5  $\mu\text{L}$  of  $\text{mg}\cdot\text{mL}^{-1}$  solution of PTh in 1:1 H<sub>2</sub>O: MeOH mixture dropped onto glassy carbon electrode surface, starting voltage of 0.0 V, ending voltage of -2.5V, 500  $\text{mV}\cdot\text{s}^{-1}$  scan rate in 0.1 M TBAPF<sub>6</sub> in DMF.

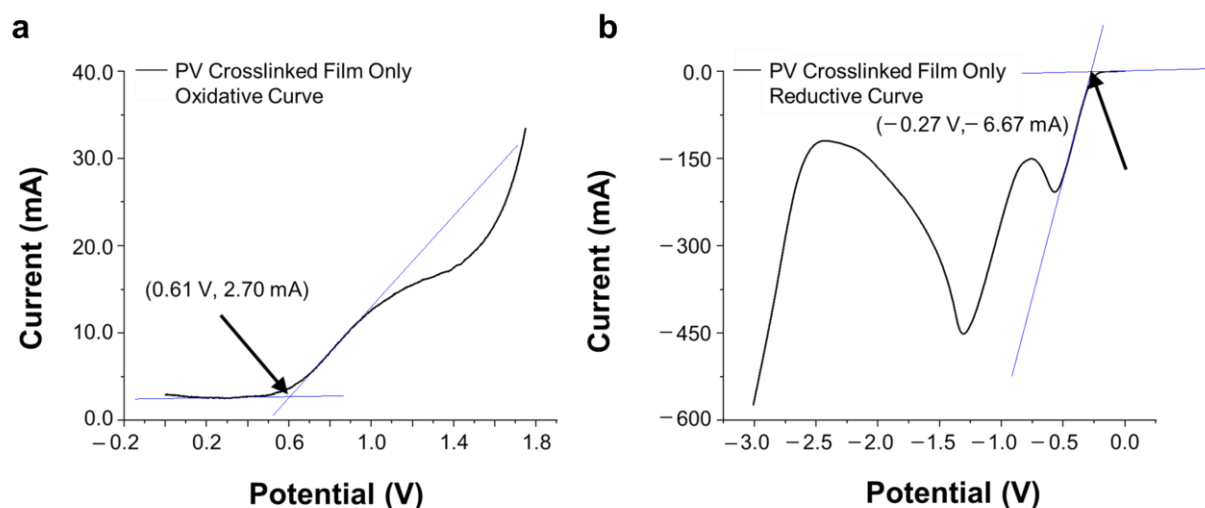


**Figure S2:** (a) Linear sweep voltammetry of PV film fabricated onto ITO slide following preparatory procedures for the 1.5  $\mu\text{m}$  PV film as working electrode, starting voltage of 0.0 V, ending voltage of 1.75 V, 500  $\text{mV}\cdot\text{s}^{-1}$  scan rate in 0.1 M TBAPF<sub>6</sub> in DMF. (b) Linear sweep voltammetry of PV film fabricated following preparatory procedures for the 1.5  $\mu\text{m}$  PV film onto ITO slide as working electrode, starting voltage of 0.0 V, ending voltage of -3.0 V, 50  $\text{mV}\cdot\text{s}^{-1}$  scan rate in 0.1 M TBAPF<sub>6</sub> in DMF.



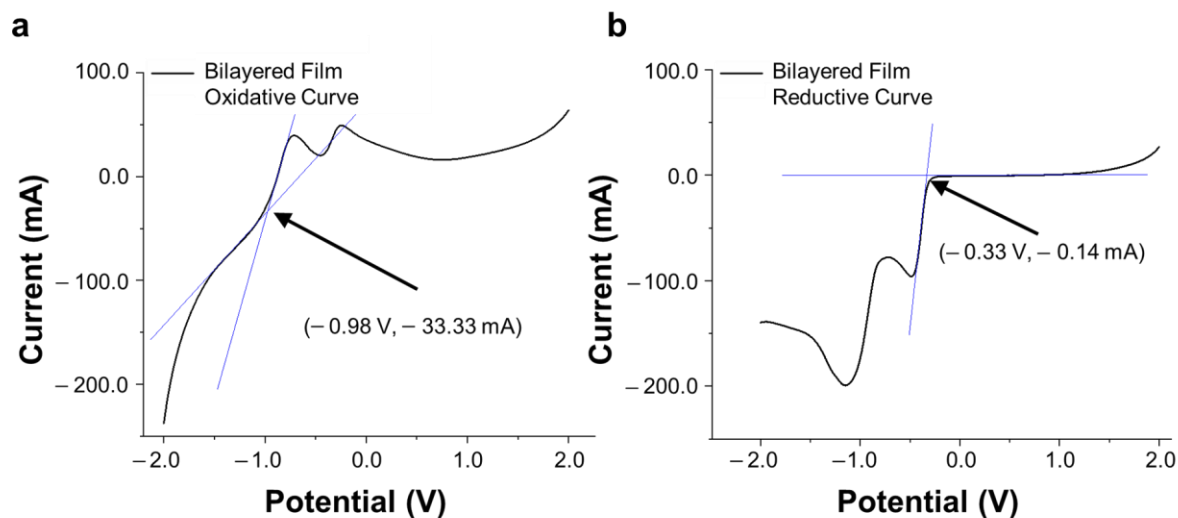


**Figure S3:** (a) Linear sweep voltammetry of bilayered film plated onto ITO slide following preparatory procedures for 0.23  $\mu\text{m}$  PTh film and 1.5  $\mu\text{m}$  PV film as working electrode, starting voltage of  $-2.0 \text{ V}$ , ending voltage of  $2.0 \text{ V}$ ,  $50 \text{ mV}\cdot\text{s}^{-1}$  scan rate in 0.1M TBAPF<sub>6</sub> in DMF. (b) Linear sweep voltammetry of bilayered film plated onto ITO slide following preparatory procedures for 0.23  $\mu\text{m}$  PTh film and 1.5  $\mu\text{m}$  PV film as working electrode, starting voltage of  $2.0 \text{ V}$ , ending voltage of  $-2.0 \text{ V}$ ,  $50 \text{ mV}\cdot\text{s}^{-1}$  scan rate in 0.1 M TBAPF<sub>6</sub> in DMF.



## Section E. Physical and Morphological Characterization of Bilayered Thin-Films

### 1) *Contact Angle Measurements*

Contact angle data was acquired by stabilizing a Samsung Note 10+ smart phone with a Clarus 15X macro lens with a tripod (**Fig S4**). A piece of white printer paper and lamp were utilized to diffuse a white LED for use as a back light. The oxidized bilayered film on a sodium silicate glass slide film was set onto a lab jack in front of the light source and the camera was positioned in front of the film. A video recording was started using the macro setting on the camera and then a 1.5  $\mu\text{L}$  drop was deposited onto the surface. The recording was stopped after 10 s. Upon review, a photo was captured at 1 s after the drop was deposited. Three drops were deposited of each solvent onto the oxidized film in differing locations and were then wicked off after the videos were captured. The films were then placed 3 in from a 450 nm (blue), 36 W light and irradiated for 1h. After this time, the process of video-capturing droplet deposition was repeated on the reduced films. Again, each drop was placed in a different location on the film. All images at 1 s after deposition were measured for contact angle in ImageJ and all  $\Theta_E$  were recorded.

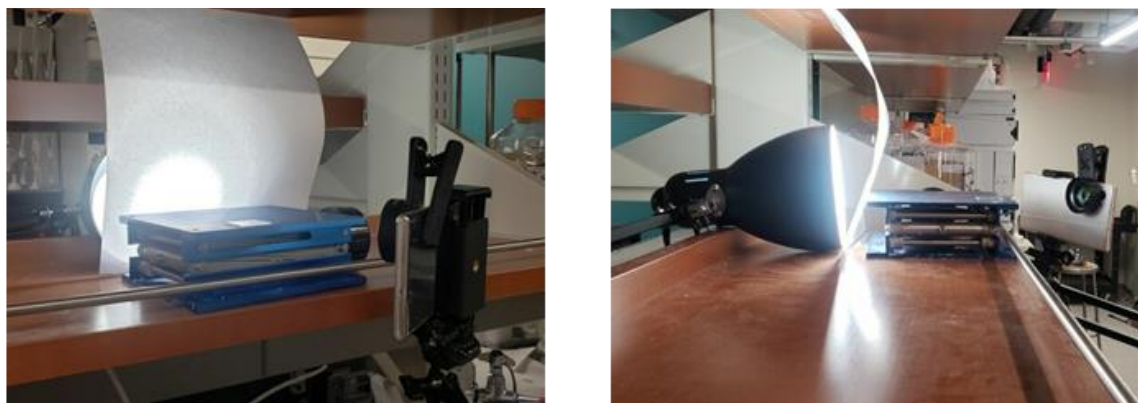


**Figure S4:** Experimental set-up for contact angle experiments. The film on its glass substrate was placed on a blue jack, acting as a stage. A desk lamp was used with a 36W white light bulb and a piece of printer paper to diffuse the light. A Samsung Note 10+ and Clarus 15X Macro Lens attachment were used to capture the video recordings of 1.5  $\mu\text{L}$  of either  $\text{H}_2\text{O}$  or MeI were dropped onto the film.



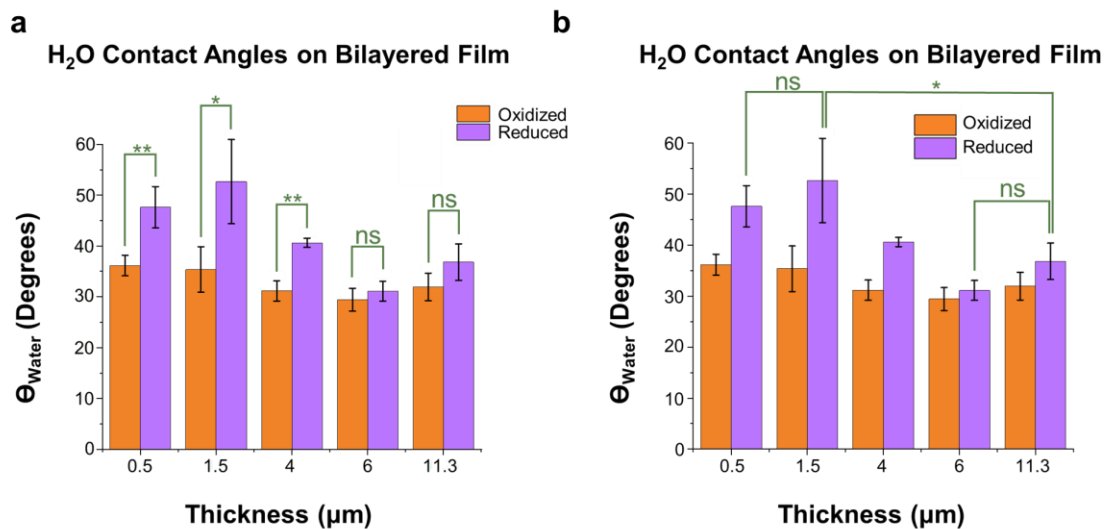


**Figure S5:** (a) H<sub>2</sub>O contact angle data before (orange) and after (purple) reduction of the PTh-PV bilayered film through irradiation with blue light. A p value of 0.0012 was found between redox states for  $0.5 \pm 0.8 \mu\text{m}$  film. A p value of 0.025 was found between redox states for  $1.5 \pm 0.6 \mu\text{m}$  film. A p value of 0.006 was found between redox states for  $4 \pm 1.0 \mu\text{m}$  film. A p value of 0.66 was found between redox states for the  $6.0 \pm 1.1 \mu\text{m}$  film. A p value of 0.29 was found for the  $11.3 \pm 1.1 \mu\text{m}$  film. (b) Same data shown in Fig. S5a, except now the statistical significance between films of different thickness is compared. H<sub>2</sub>O droplet contact angle measurements with calculated p-values between different thicknesses. A p value of 0.0107 was determined between the  $1.5 \pm 0.6 \mu\text{m}$  films and the  $11.3 \pm 1.1 \mu\text{m}$  films. No significance was determined for the difference between  $0.5 \pm 0.08 \mu\text{m}$  films and the  $1.5 \pm 0.6 \mu\text{m}$  films (p value = 0.4731). No significance was determined for the difference between the  $1.5 \pm 0.6 \mu\text{m}$  films and the  $11.3 \pm 1.1 \mu\text{m}$  (p value = 0.088).

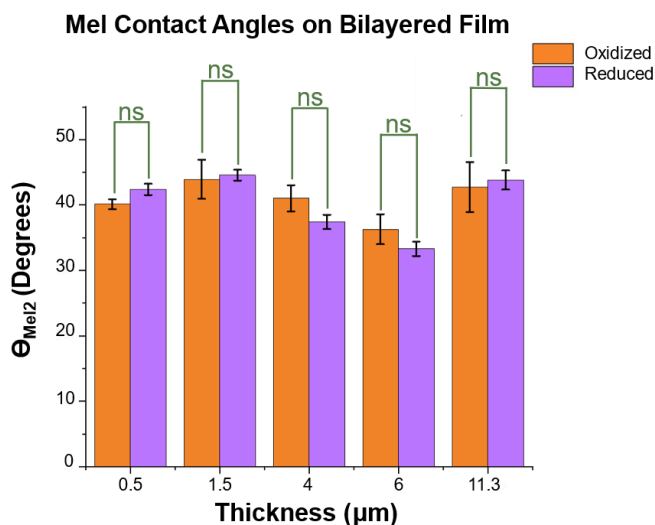


**Figure S6:** Mel contact angle experiments. No significance was determined between the oxidized and reduced forms of the film.



## 2) Profilometry

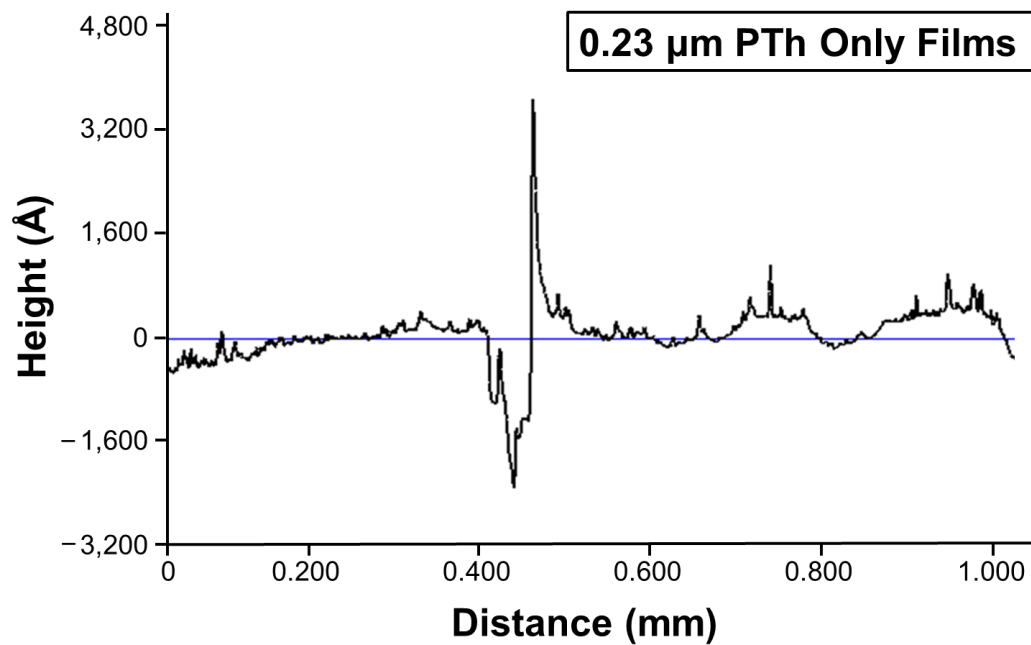


**Figure S7:** Profilometry run for PTh only layer with an average thickness of  $0.23 \pm 0.03 \mu\text{m}$ .

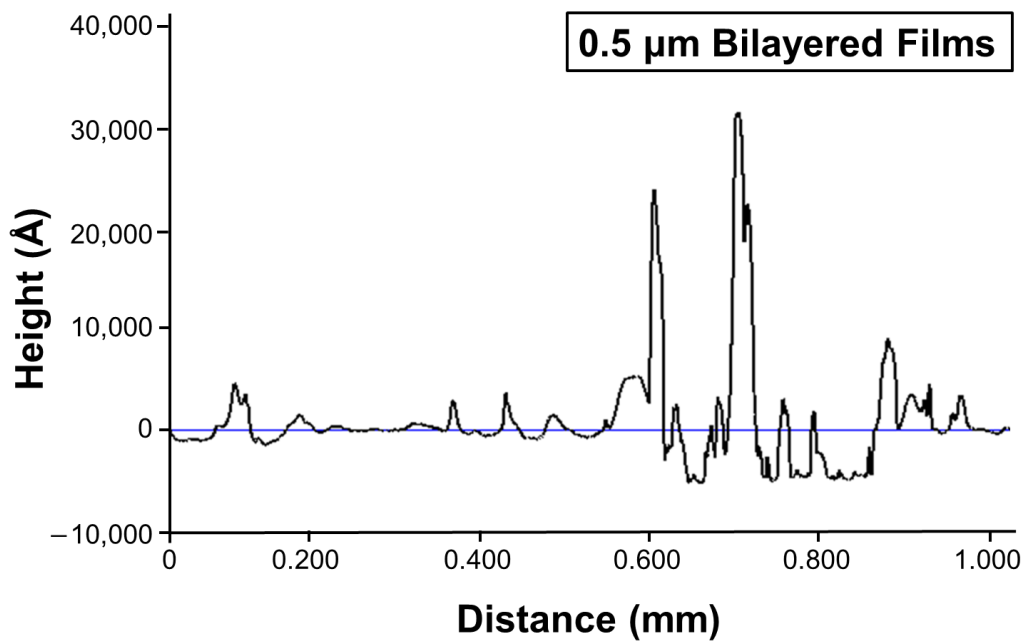


**Figure S8:** Profilometry run for bilayered film with an average thickness of  $0.5 \pm 0.08 \mu\text{m}$ .



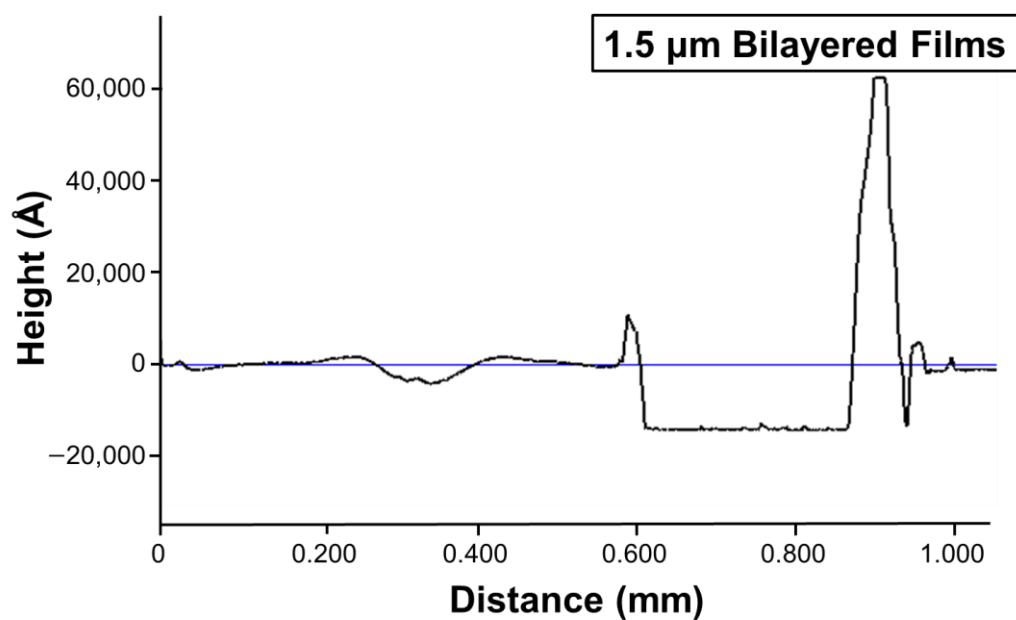


**Figure S9:** Profilometry run for bilayered film with an average thickness of  $1.5 \pm 0.6 \mu\text{m}$ .

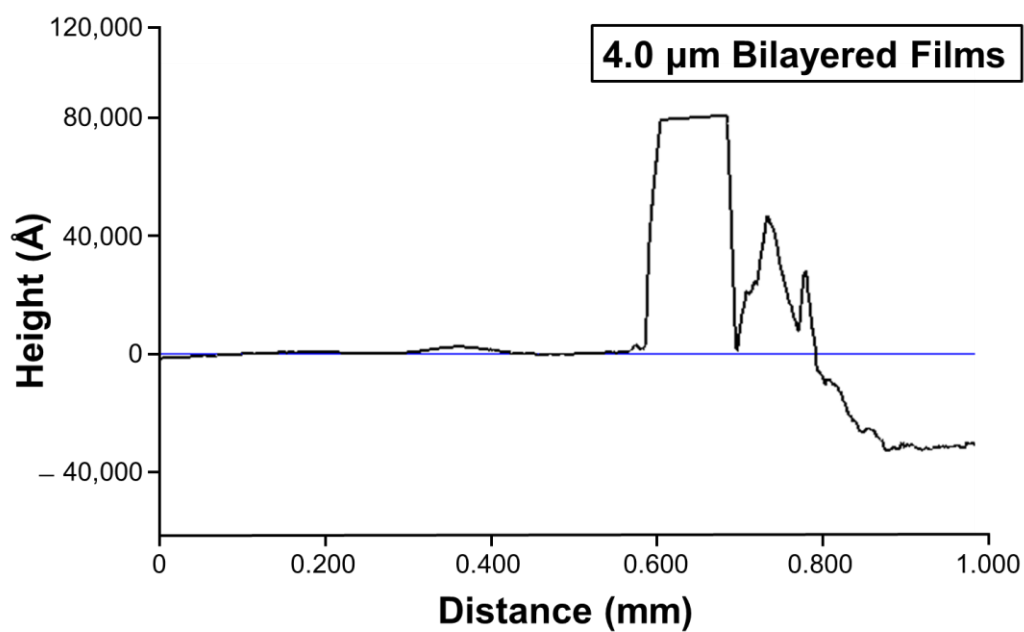


**Figure S10:** Profilometry run for bilayered film with an average thickness of  $4.0 \pm 0.8 \mu\text{m}$ .



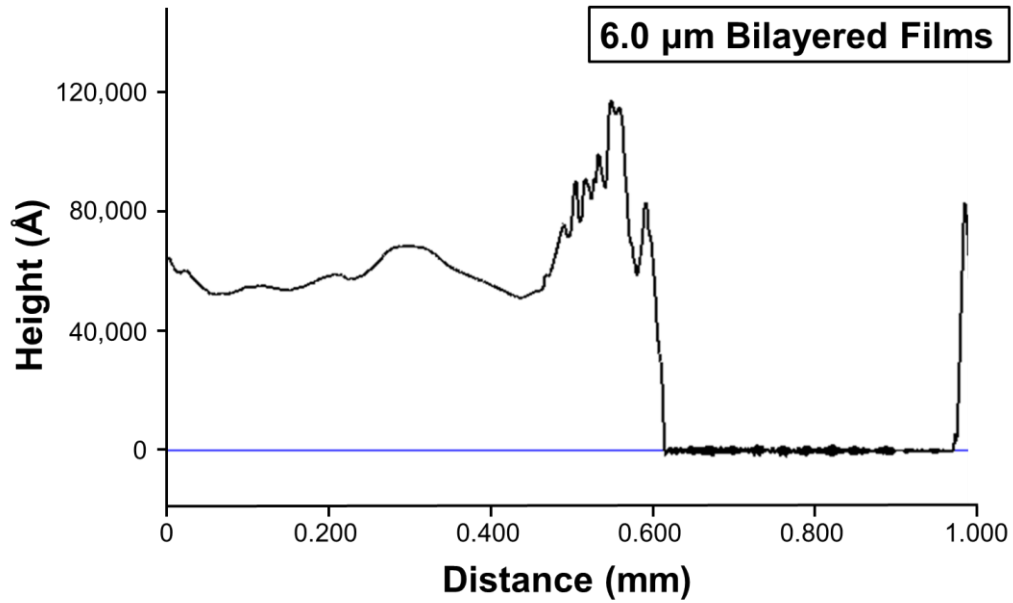


**Figure S11:** Profilometry run for bilayered film with an average thickness of  $6.0 \pm 1.0 \mu\text{m}$ .

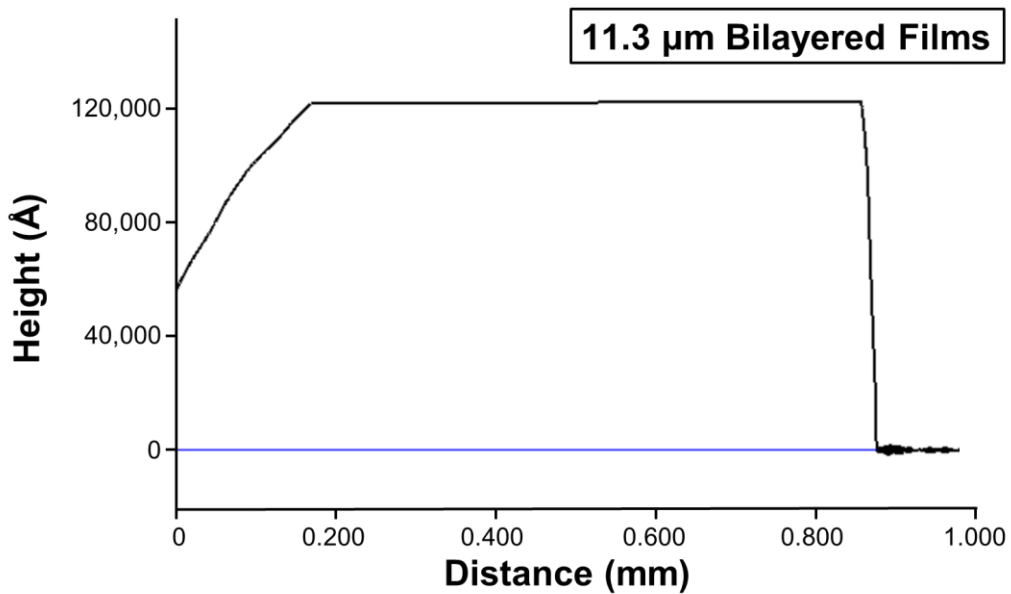


**Figure S12:** Profilometry run for bilayered film with an average thickness of  $11.3 \pm 1.0 \mu\text{m}$ .



### 3) Atomic Force Microscopy

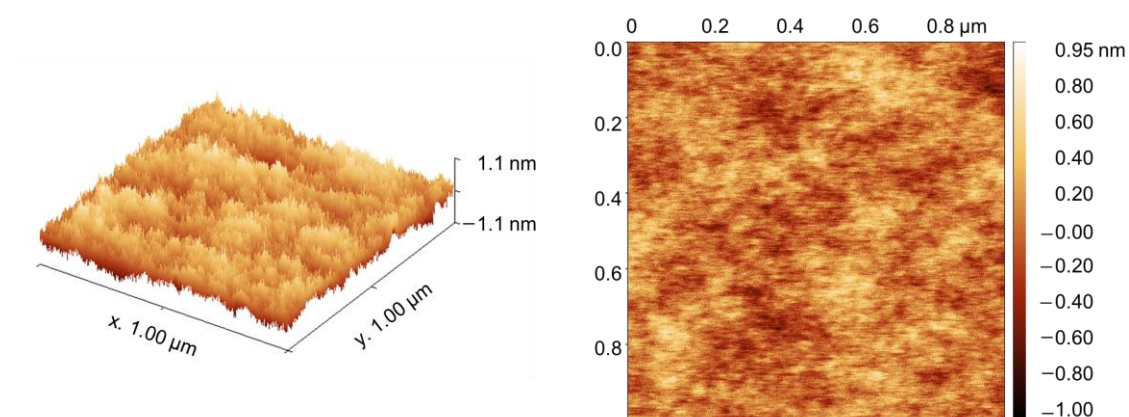


**Figure S13:** AFM data on a 1 μm scale for the  $1.5 \pm 0.6$  μm bilayered film.

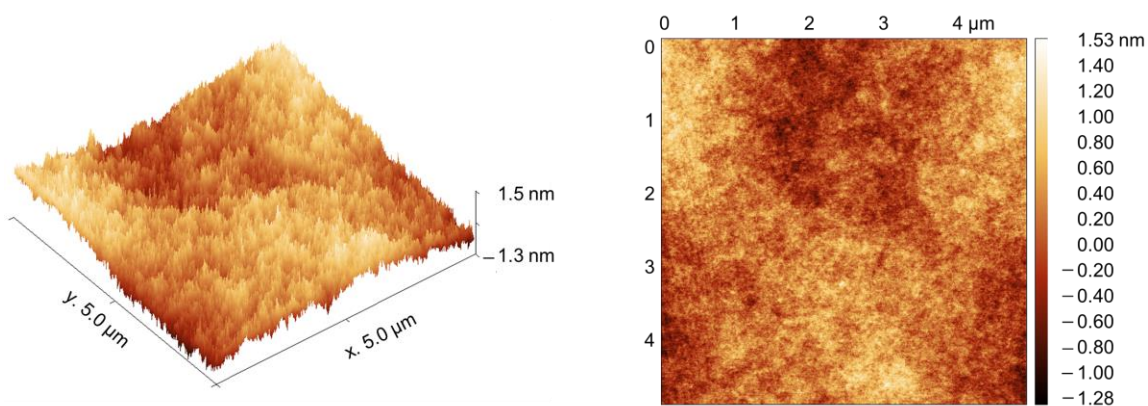


**Figure S14:** AFM data on a 5 μm scale for the  $1.5 \pm 0.6$  μm bilayered film



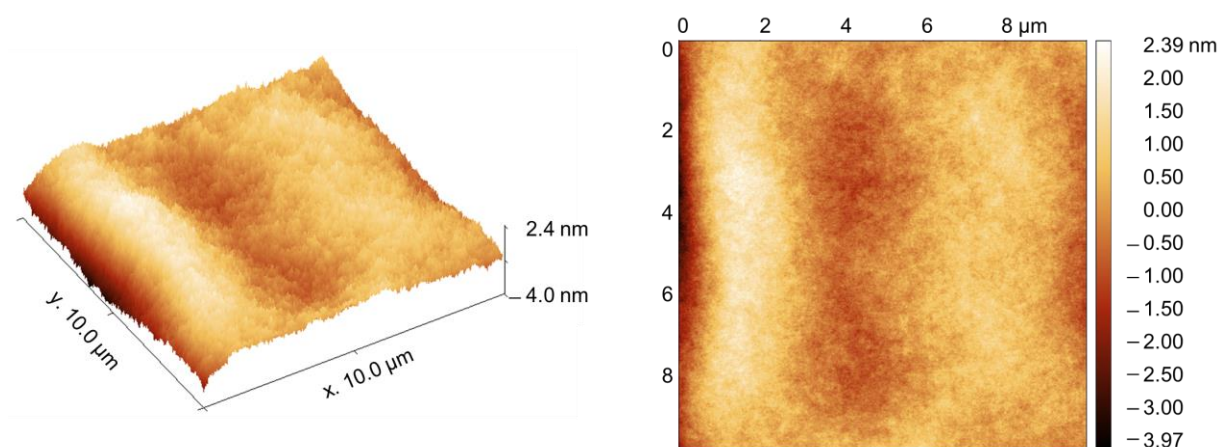


**Figure S15:** AFM data on a 10  $\mu\text{m}$  scale for the  $1.5 \pm 0.6 \mu\text{m}$  bilayered film.

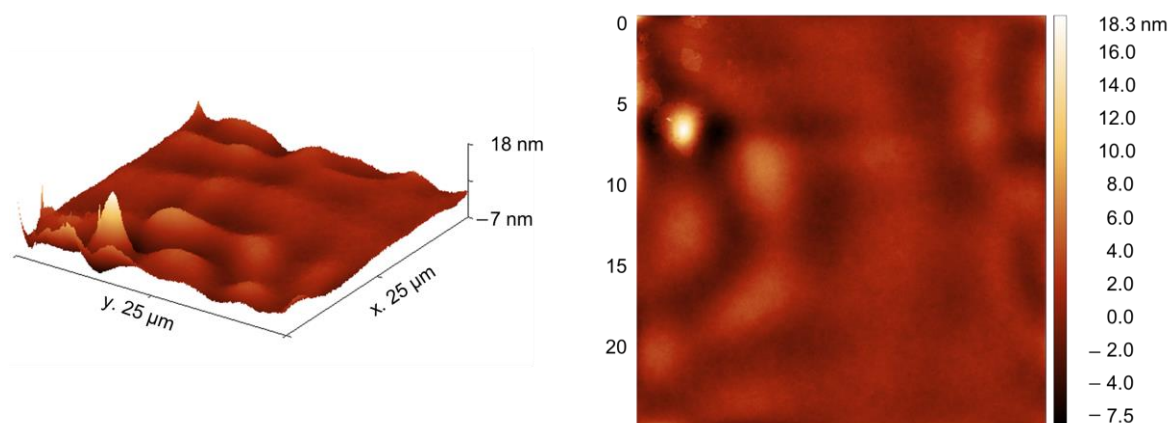


**Figure S16:** AFM data on a 25  $\mu\text{m}$  scale for the  $1.5 \pm 0.6 \mu\text{m}$  bilayered film.

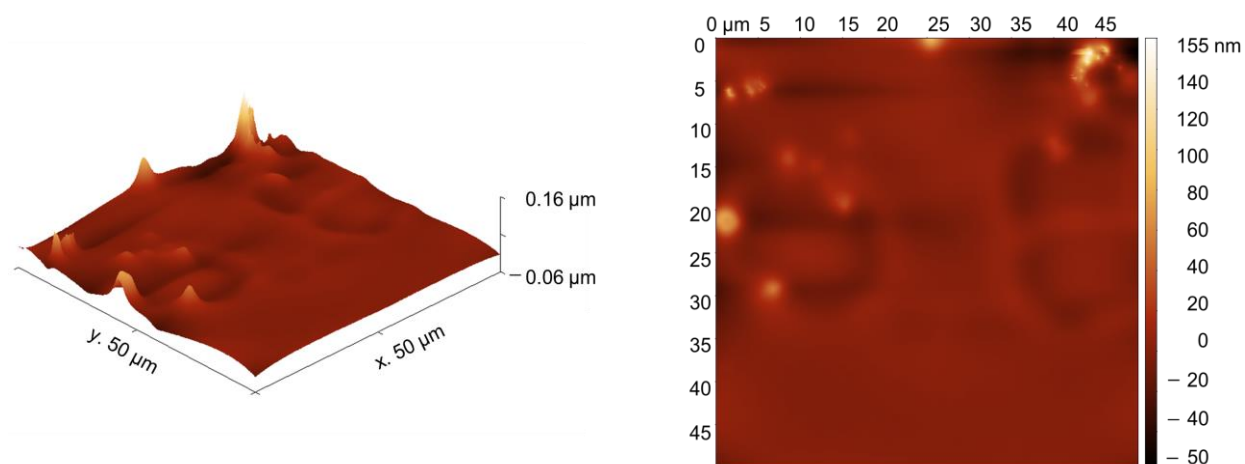


**Figure S17:** AFM data on a 50  $\mu\text{m}$  scale for the  $1.5 \pm 0.6 \mu\text{m}$  bilayered film.



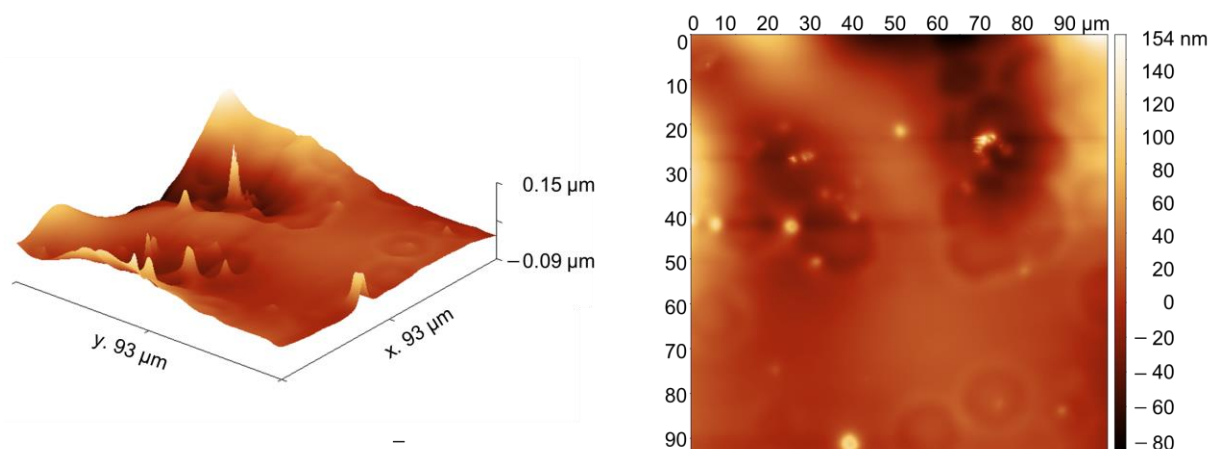


**Figure S18:** AFM data on a 100  $\mu\text{m}$  scale for the  $1.5 \pm 0.6 \mu\text{m}$  bilayered film.

#### 4) Scanning Electron Microscopy

### 5,000 X Magnification

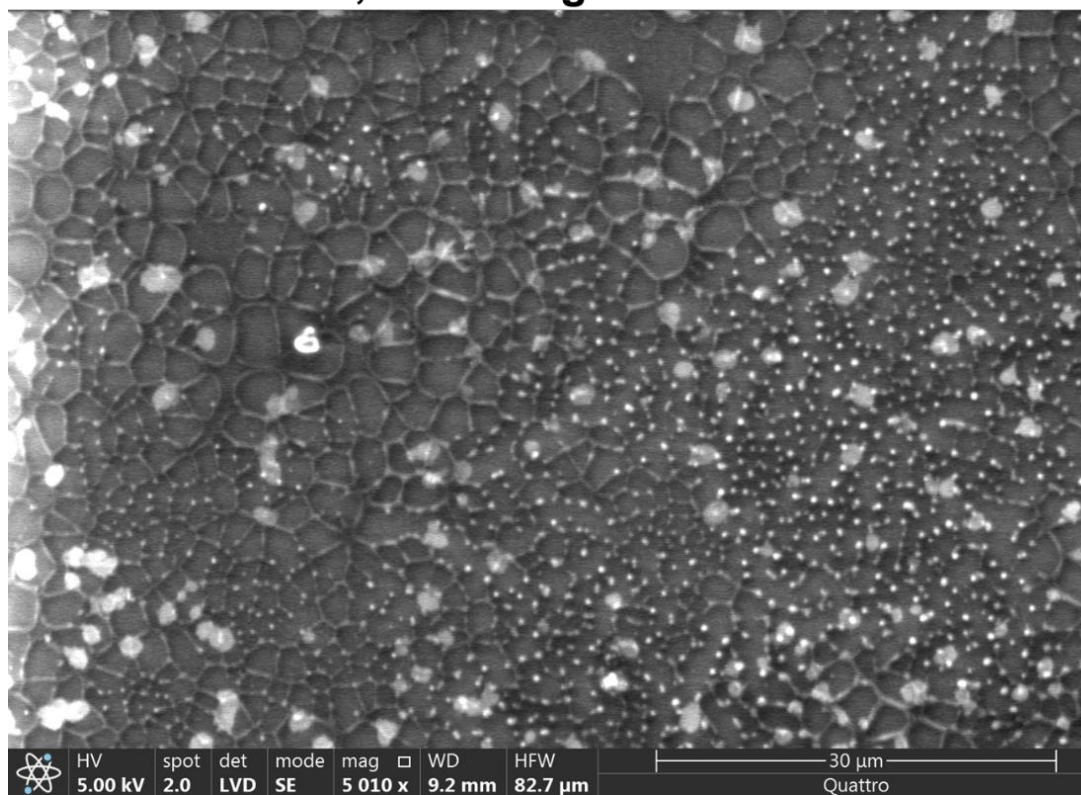


**Figure S19:** Low-vacuum SEM image of  $1.5 \pm 0.6 \mu\text{m}$  bilayered film at 5,000 X magnification.



## 5) Gel Permeation Chromatography

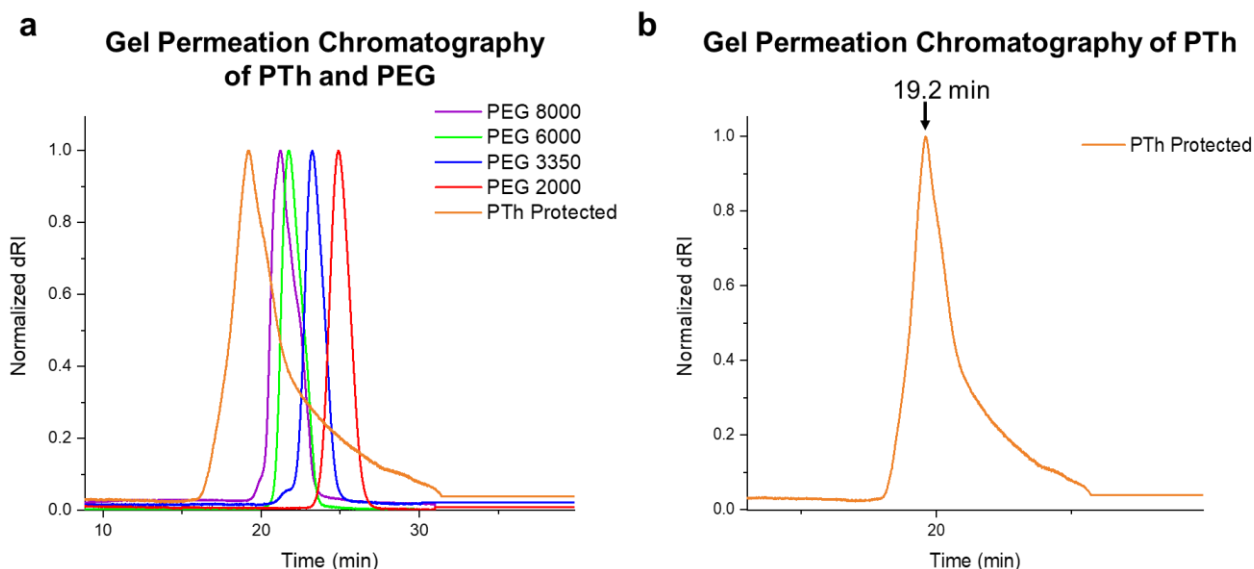


**Figure S20:** (a) Gel permeation chromatography normalized spectra of 10 mg·mL<sup>-1</sup> solutions of the ester protected PTh and 4 different polyethylene glycol (PEG) molecular weights. The PTh was left protected to ensure solubility on the DMF preparatory GPC column. The PEG was run to establish a calibration curve that could be used to give an approximate  $M_p$  as well as a  $DP_n$  for the PTh. (b) The PTh GPC data with notation showing the peak time elution.

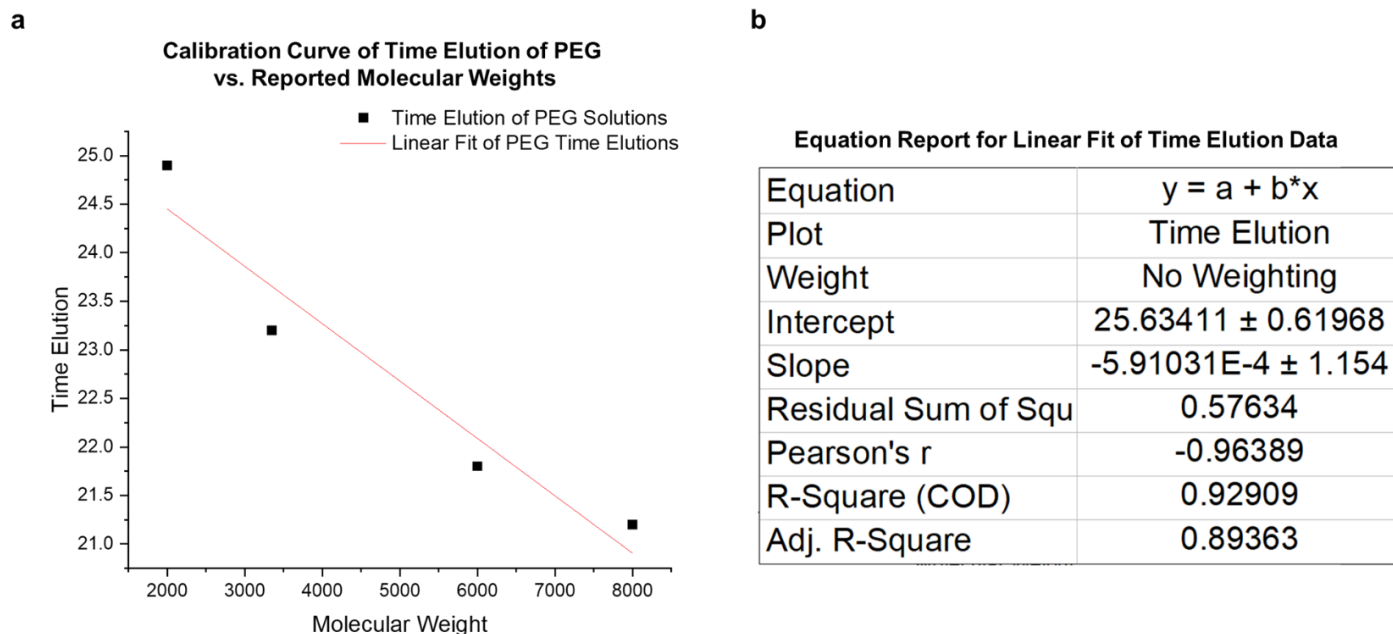


**Figure S21:** (a) The calibration curve compiled from the time elution data vs the molecular weight of the run PEG chains. Red line shows the linear fit used to approximate  $M_p$  of the protected PTh. (b) Table shows the equation with determined variables that were used to calculate an  $M_p$  of 10,800 for the protected PTh. This informs a  $DP_p$  of 36.



6)  $^1\text{H}$  NMR Spectroscopy

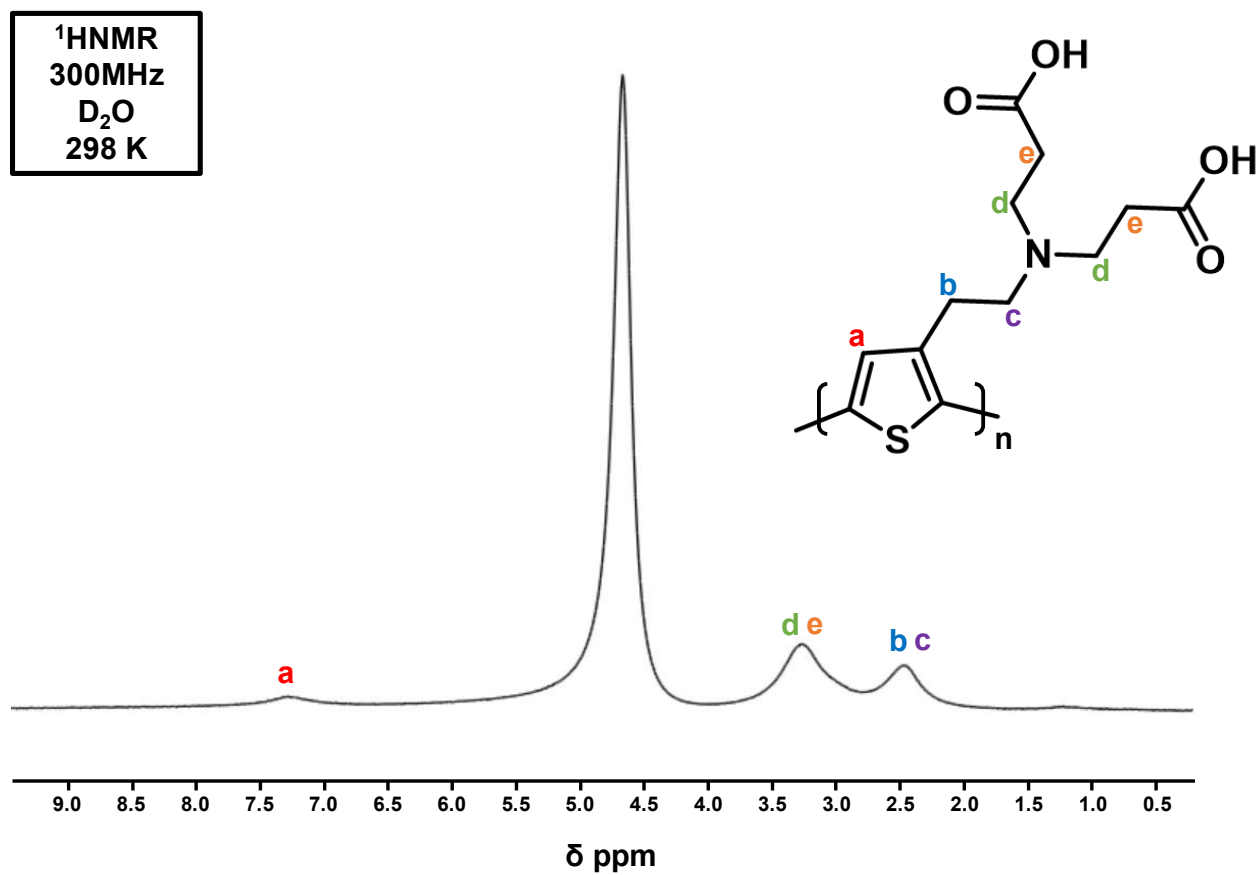


**Figure S22:**  $^1\text{H}$  NMR spectroscopy on a 300 MHz Variant Spectrometer of the final PTh in  $\text{D}_2\text{O}$ .



## Section F. UV-Vis-NIR Absorption / Photoluminescence Spectroscopy

### 1) UV-Vis-NIR Absorption Spectra

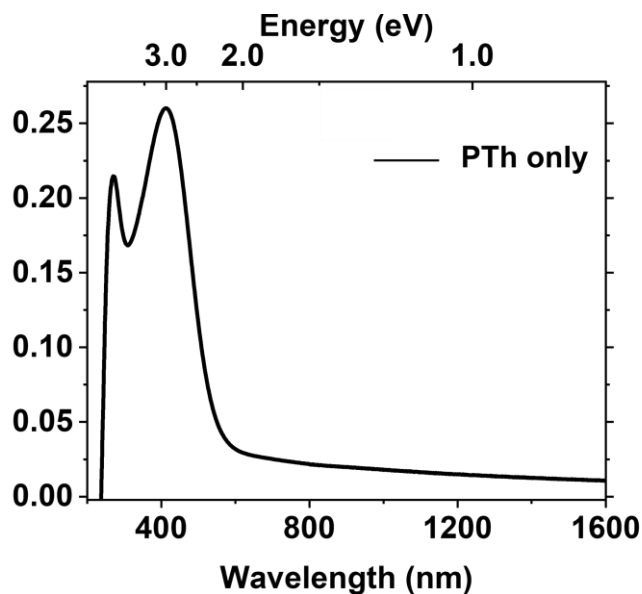


**Figure S23:** UV-Vis Spectroscopy of  $0.23 \pm 0.03 \mu\text{m}$  PTh only on sodium silicate microscope slide from a wavelength of 200 nm to 1,600 nm. Onset of peak is labelled with arrow.

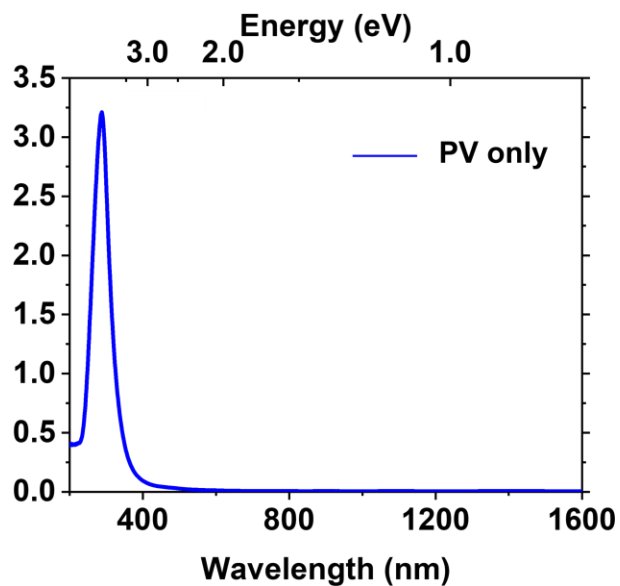


**Figure S24:** UV-Vis Spectroscopy of  $1.5 \pm 0.6 \mu\text{m}$  PV crosslinked film only on sodium silicate microscope slide from a wavelength of 200 nm to 1,600 nm. Onset of peak is labelled with arrow.



## 2) Photoluminescence Spectra

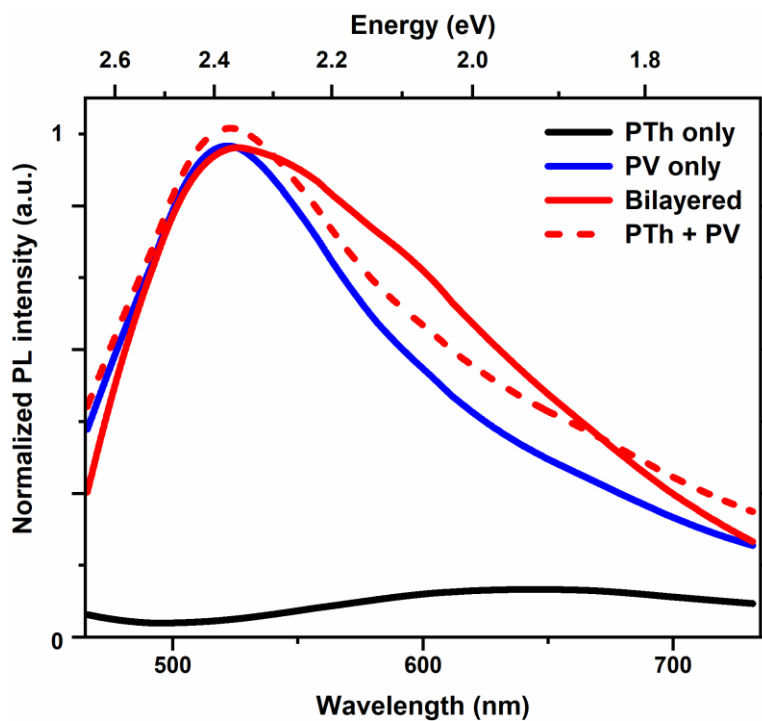


**Figure S25:** PL spectra excited at 420 nm (2.95 eV) of PTh only film (black),  $1.5 \pm 0.6 \mu\text{m}$  PV film only (blue), the bilayered film with  $1.5 \pm 0.6 \mu\text{m}$  PV layer (red), and the sum of the PTh and PV layers (red dash) on sodium silicate microscope slide from 1.6 eV to 2.75 eV.



## Section G. Femtosecond Transient Absorption Spectroscopy

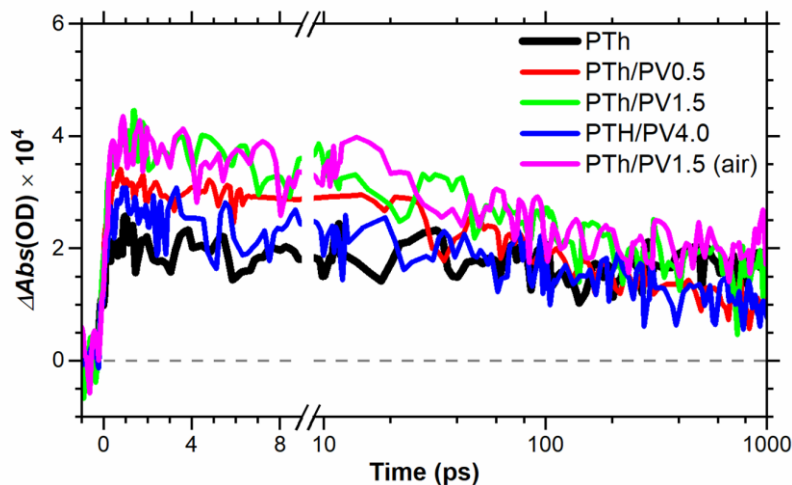


**Figure S26:** The temporal profiles of the induced-absorption signals at a probe energy ( $E_{\text{A1}}$ ) of 1.72 eV recorded using  $E_{\text{ex}} = 2.48$  eV for the PTh bottom layer (black) and bilayered samples PTh/PV0.5 (red), PTh/PV1.5 (green), PTh/PV4.0 (blue), and PTh/PV1.5 open to air (magenta) appear within the instrument response function and are long lived.

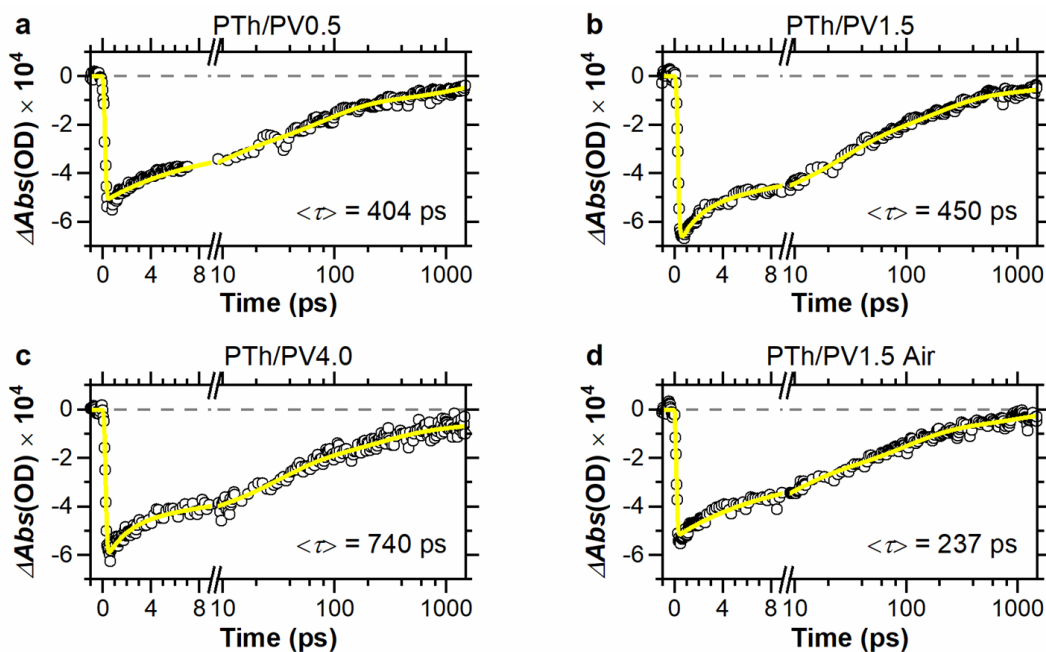


**Figure S27:** The temporal profiles of the BL signals recorded at a probe energy ( $E_{\text{BL}}$ ) of 2.38 eV for the bilayered samples of PTh/PV0.5 (a), PTh/PV1.5 (b), and PTh/PV4.0 (c) are plotted as open circles. These data were collected using  $E_{\text{ex}} = 2.48$  eV while purging the films with nitrogen. The temporal profile of the PTh/PV1.5 bilayered in air at the same probe energy is plotted in (d). Each of the profiles was fit (yellow) to a sum of a single exponential rise and multiple decays convoluted with a 200 fs instrument response function. The time constants and average decay lifetimes obtained are included. Table S1 and S2.



### 1) Fitting of Temporal Profiles

The temporal profiles recorded at specific energies within the fTA data were fit to a sum of a single-exponential rise and multiple exponential decays convoluted with a Gaussian instrument response function (IRF) with a breadth of 200 fs. Specifically, the fitting function used is:

$$\Delta Abs(E, t) = IRF \otimes \left[ \sum_{n=1}^4 \left( A_i \exp\left(-t/\tau_i\right) \right) - A_{rise} \exp\left(-t/\tau_{rise}\right) \right].$$

The  $\tau_i$  values are the exponential decay time constants,  $\tau_{rise}$  is the exponential rise time constant, and  $A_i$  and  $A_{rise}$  are the amplitudes of each exponential term. These parameters were used as fitting parameters, and up to four exponential decays were utilized. The uncertainties of these parameters represent values obtained in the fitting, and they are not errors based on multiple measurements. Note, each bilayered film was purged with N<sub>2</sub> unless otherwise indicated.

**Table S1.** Time constants (in ps) obtained by fitting the temporal profiles of the bleach signals at a probe energy ( $E_{BL}$ ) of 2.38 eV in the fTA data collected using  $E_{ex} = 2.48$  eV.

Time Constants (ps)	PTh/PV0.5	PTh/PV1.5	PTh/PV4.0	PTh/PV1.5 (Air)	PTh
$\tau_{rise}$	0.05(1)	0.085(7)	0.07(1)	0.06(1)	0.101(7)
$\tau_1$	6.9(1)	1.67(9)	1.7(1)	7.6(2)	0.96(7)
$\tau_2$	75.0(6)	22.4(3)	27.5(6)	92(1)	17.5(3)
$\tau_3$	1663(9)	175(2)	232(7)	1160(10)	137.3(8)
$\tau_4^*$	— —	3260(70)	4500(300)	— —	4400(60)
$\tau_{Average}$	404(7)	450(30)	740(80)	237(5)	760(80)

\* The TA data were collected over a 1.5 ns long window. As a result, the uncertainty of these long lifetime components are therefore likely higher than the values obtained from the fitting of these single measurements.

**Table S2.** Decay time constants (in ps) obtained by fitting the temporal profiles at  $E_{BL} = 2.38$  eV and  $E_{IA2} = 1.97$  eV for the different samples. The lifetimes for the bleach profiles at 2.38 eV are average lifetimes calculated using the data in Table S1. These profiles are associated with  $E_{BL}$ , which corresponds to the PTh being in an excited or charged state. The temporal profiles at 1.97 eV were obtained by subtracting the temporal profile of the PTh film from the profile of the indicated bilayered film at that energy. These profiles are associated with  $E_{IA2}$  and the presence of electrons in the PV acceptor film, which were each fit to a single-exponential decay.

Energy	Probe Energy (eV)	PTh/PV0.5	PTh/PV1.5	PTh/PV4.0	PTh/PV1.5 (Air)	PTh
$E_{BL}$	2.38	404(7)	450(30)	740(80)	237(5)	760(80)
$E_{IA2}$	1.97	167(1)	140(1)	204(1)	106(1)	— —



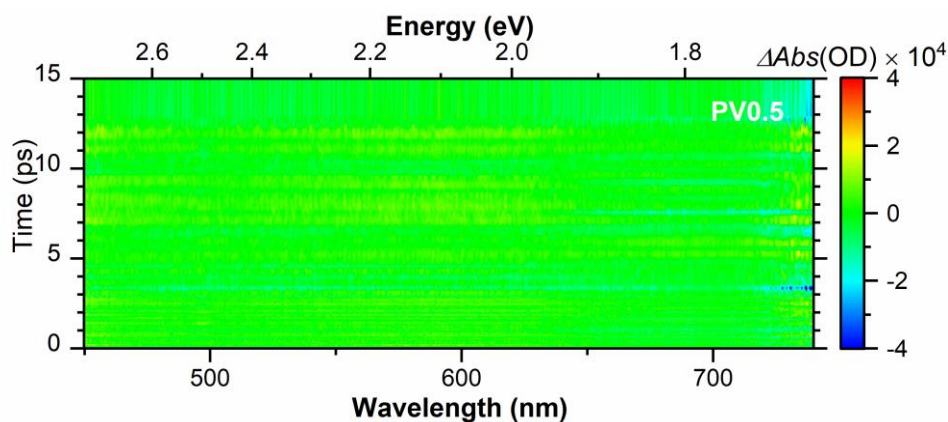


**Figure S28:** fTA data collected on the PV0.5 electron-acceptor film using  $E_{ex} = 2.48$  eV (500 nm). Since there is negligible absorption at this photon energy, there are no transient absorption signals detectable.

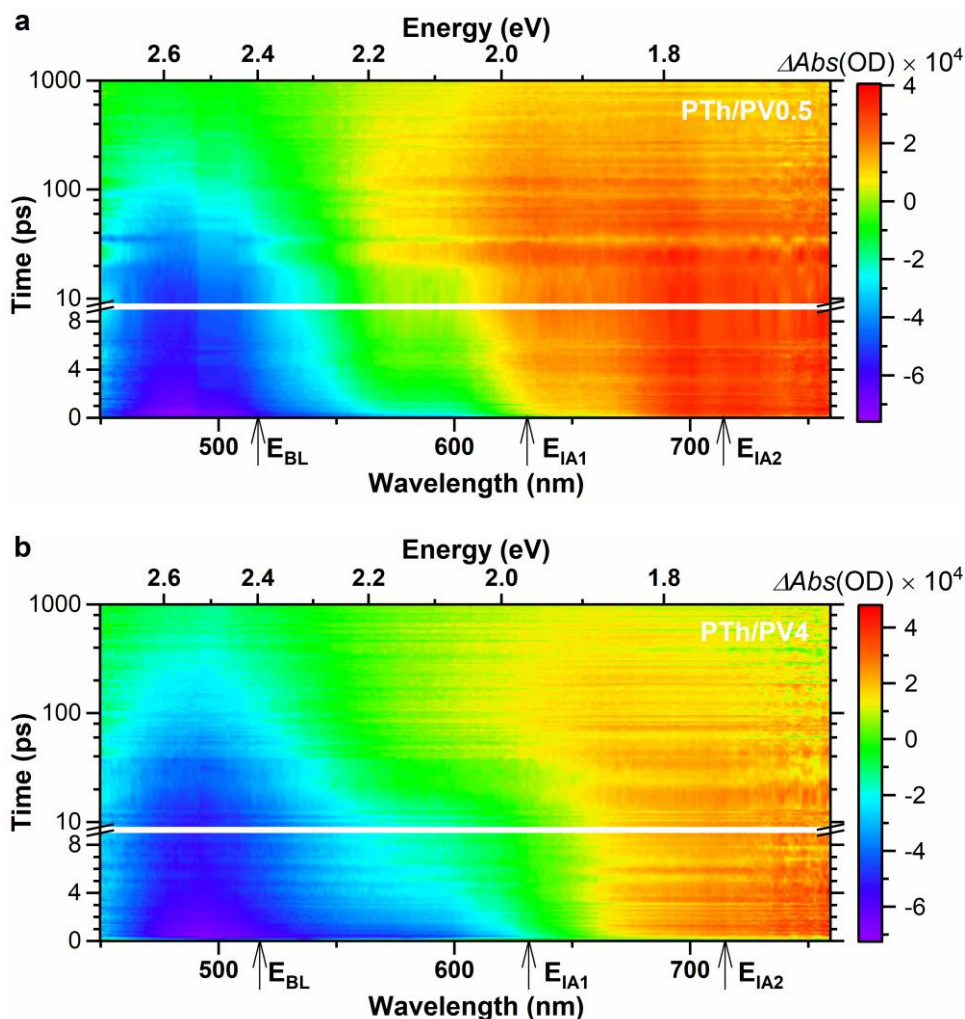


**Figure S29:** fTA data collected on the PTh/PV0.5 (a) and PTh/PV4.0 (b) bilayered films using  $E_{ex} = 2.48$  eV (500 nm). The temporal profiles of the bleach signals recorded at a probe energy  $E_{BL} = 2.38$  eV are included in Fig. S24. The temporal profiles of the induced-absorption signals at  $E_{IA1} = 1.72$  eV are included in Fig. S23.



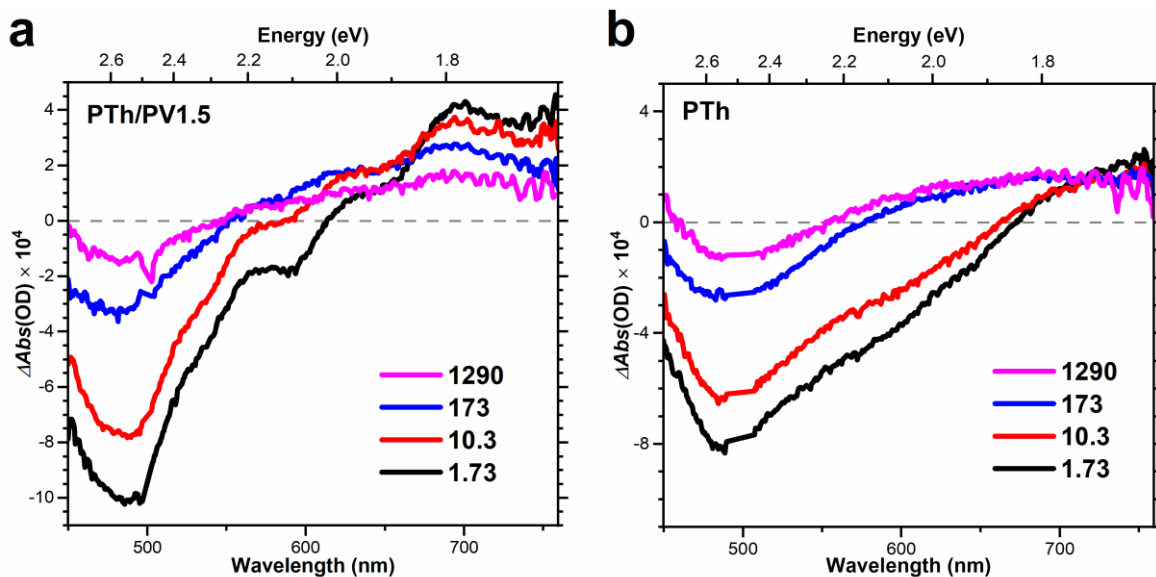


**Figure S30:** (a) fTA spectra collected for the PTh/PV1.5 bilayered film with  $E_{\text{ex}} = 2.48$  eV at time (ps) 1290, 173, 10.3, and 1.73. Similar data are presented in (b) displaying the fTA data for the PTh bottom layer film.

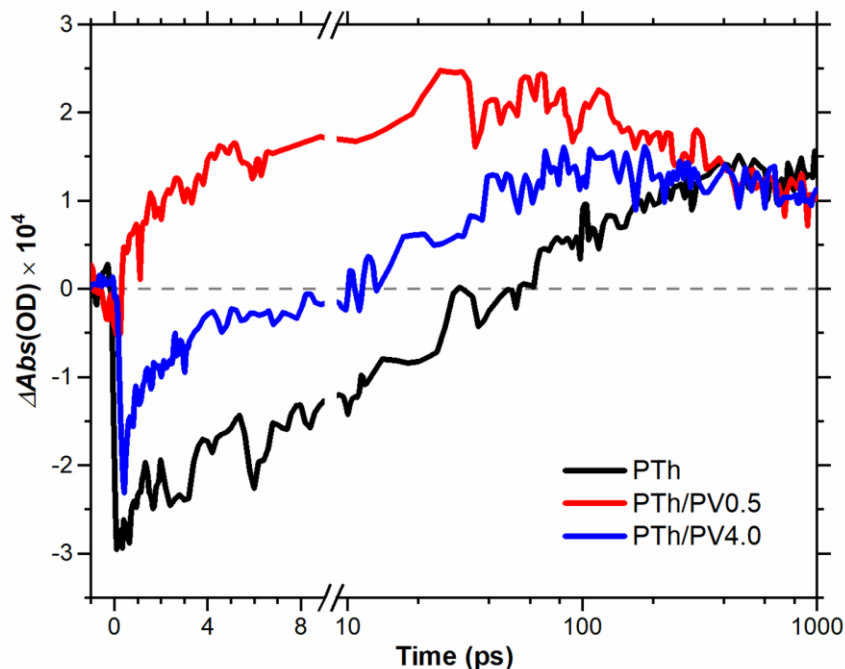


**Figure S31:** The temporal profiles of the fTA data at  $E_{\text{A2}} = 1.97$  eV for PTh (black), PTh/PV0.5 (red), and PTh/PV4.0 (blue) collected using  $E_{\text{ex}} = 2.48$  eV. The profiles are complicated due to overlapping bleach and induced-absorption signals.



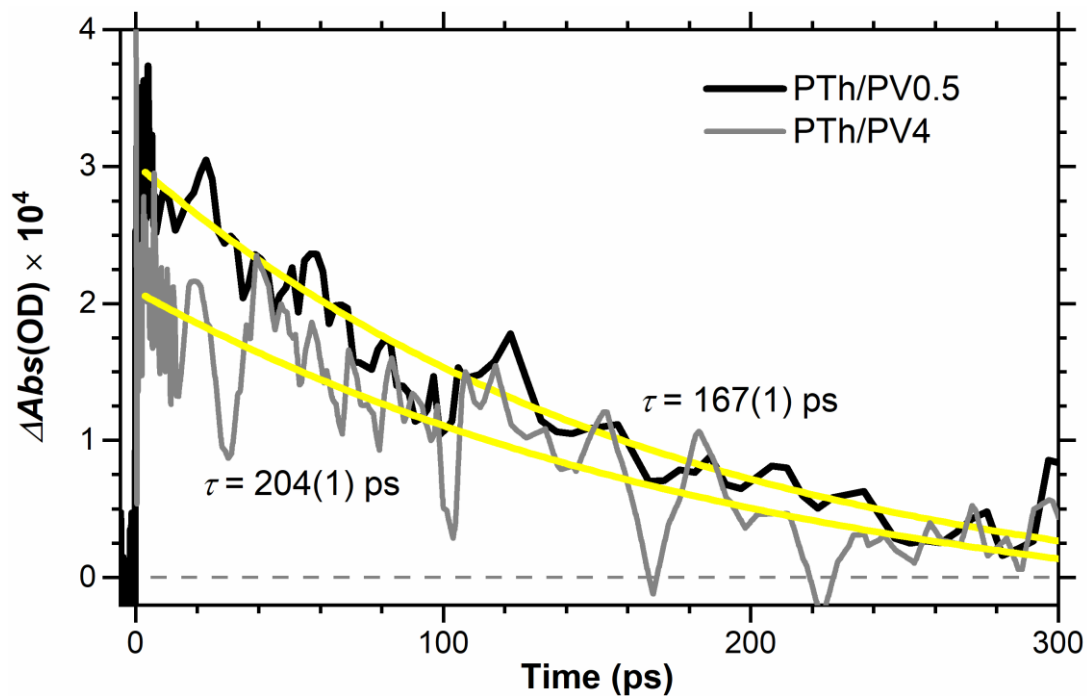


**Figure S32:** Temporal profile of the electron occupancy in the PV0.5 (black) and PV4 (gray) acceptor layers estimated by subtracting the temporal profile at  $E_{A2}=1.97$  eV in the fTA data of the PTh sample from the profile of the PTh/PV0.5 and PTh/PV4 sample at the same energy. The electron occupancy profile obtained was fit to a single-exponential decay (yellow curves) with a lifetime of 167(1) ps for the PV0.5 sample and 204(1) ps for the PV4 sample.



## 2) Dependence of fTA data on Excitation Fluence

Most of the fTA data were collected using  $E_{ex} = 2.48$  eV (or  $4 \times 10^{-19}$  J) and an energy density of  $\sim 50 \mu\text{J cm}^{-2} \text{ pulse}^{-1}$ . The resultant excitation fluence is then:

$$(\sim 50 \mu\text{J cm}^{-2} \text{ pulse}^{-1}) / (4 \times 10^{-19} \text{ J}) = 1.25 \times 10^{14} \text{ cm}^{-2} \text{ pulse}^{-1}.$$

This fluence is quite low, and carrier-carrier interactions and heating are expected to be minimal. Additional fTA data were collected using higher fluences to verify this assumption. Data collected using a fluence  $\sim 2.5\times$  higher are included in **Fig. S30**.

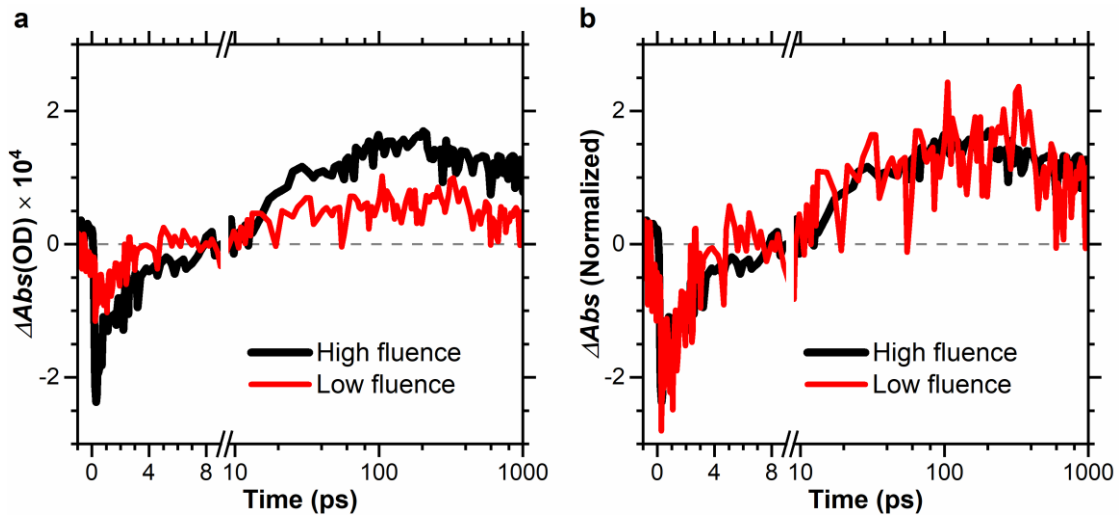


**Figure S33.** Excitation-fluence dependence of the fTA data collected on the PTh/PV4.0 bilayered sample. The temporal profiles at an energy of  $E_{IA2} = 1.97$  eV were collected with  $E_{ex} = 2.48$  eV and a fluence of  $\sim 1.25 \times 10^{14} \text{ cm}^{-2} \text{ pulse}^{-1}$  (red) and  $\sim 2.5\times$  higher (black). The acquired fTA data is in (a), and the low fluence profile is scaled to the high-fluence profile in (b). No discernable differences in the profiles are recognized.



### 3) Dependence of fTA Data on Excitation Time

In order to probe for charging or photo-induced changes in the PTh/PV1.5 bilayered sample, fTA data were recorded continuously over a period of 3 h. The fTA spectrum at  $t = 2$  and 270 ps acquired in the first and last acquisition are plotted in **Fig. S31**. The spectra collected in the first acquisition (black and red) are nearly identical to the spectra collected after 3 h (green and blue). We conclude there are no changes in the sample.

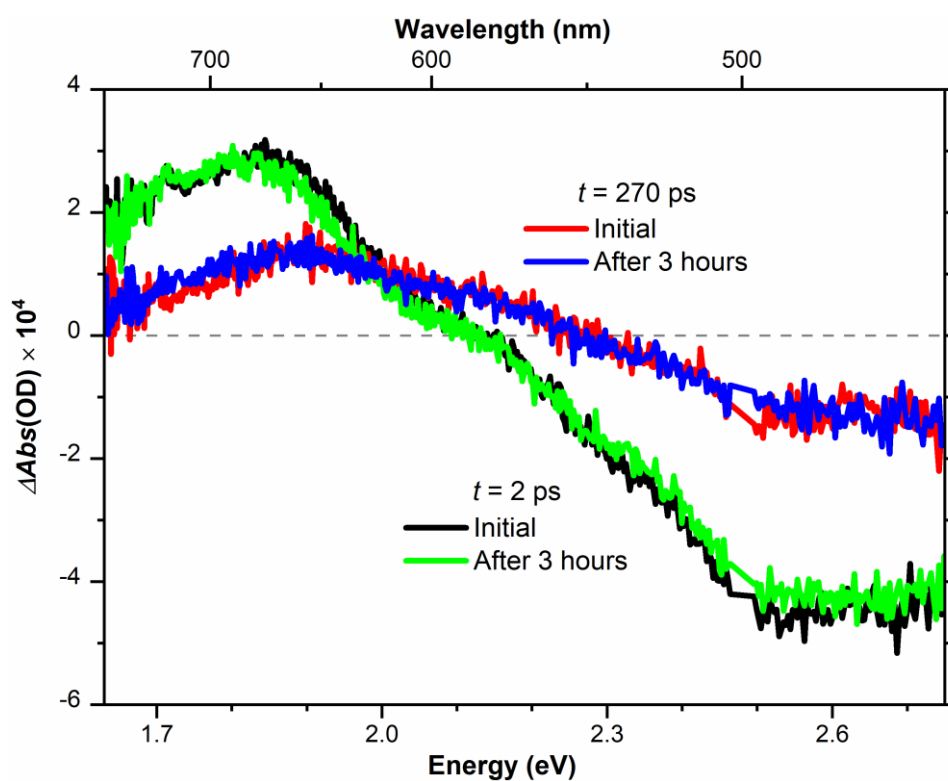


**Figure S34.** Stability test of the PTh/PV1.5 bilayered sample. fTA spectra at  $t = 2$  ps and 270 ps collected using  $E_{ex} = 2.48$  eV.



## Section H. References

1. Greene, A. F.; Danielson, M. K.; Delawder, A. O.; Liles, K. P.; Li, X.; Natraj, A.; Wellen, A.; Barnes, J. C., Redox-Responsive Artificial Molecular Muscles: Reversible Radical-Based Self-Assembly for Actuating Hydrogels. *Chem. Mater.* **2017**, 29 (21), 9498-9508.
2. Amir, F.; Liles, K. P.; Delawder, A. O.; Colley, N. D.; Palmquist, M. S.; Linder, H. R.; Sell, S. A.; Barnes, J. C., Reversible Hydrogel Photopatterning: Spatial and Temporal Control over Gel Mechanical Properties Using Visible Light Photoredox Catalysis. *ACS Appl. Mater. & Interfaces* **2019**, 11 (27), 24627-24638.
3. Ionescu, A.; Cornut, D.; Soriano, S.; Guissart, C.; Van Antwerpen, P.; Jabin, I., Efficient 'one-pot' methodology for the synthesis of novel tetrahydro- $\beta$ -carboline, tetrahydroisoquinoline and tetrahydrothienopyridine derivatives. *Tetrahedron Lett.* **2013**, 54 (45), 6087-6089.
4. Xing, C.; Xu, Q.; Tang, H.; Liu, L.; Wang, S., Conjugated Polymer/Porphyrin Complexes for Efficient Energy Transfer and Improving Light-Activated Antibacterial Activity. *J. Am. Chem. Soc.* **2009**, 131 (36), 13117-13124.